#70156

(47)

LA-UR-96-1848 DRAFT I - 052296

DETERMINATION OF AN IN-SITU VADOSE ZONE VAPOR PHASE DIFFUSION COEFFICIENT AT A MESA TOP WASTE DISPOSAL FACILITY

Erik Vold[1] and Bart Eklund[2]

1. Los Alamos National Laboratory, Los Alamos, NM

2. RADIAN Corp., Austin, TX

Received by EH-RPF

OCT 10 2001

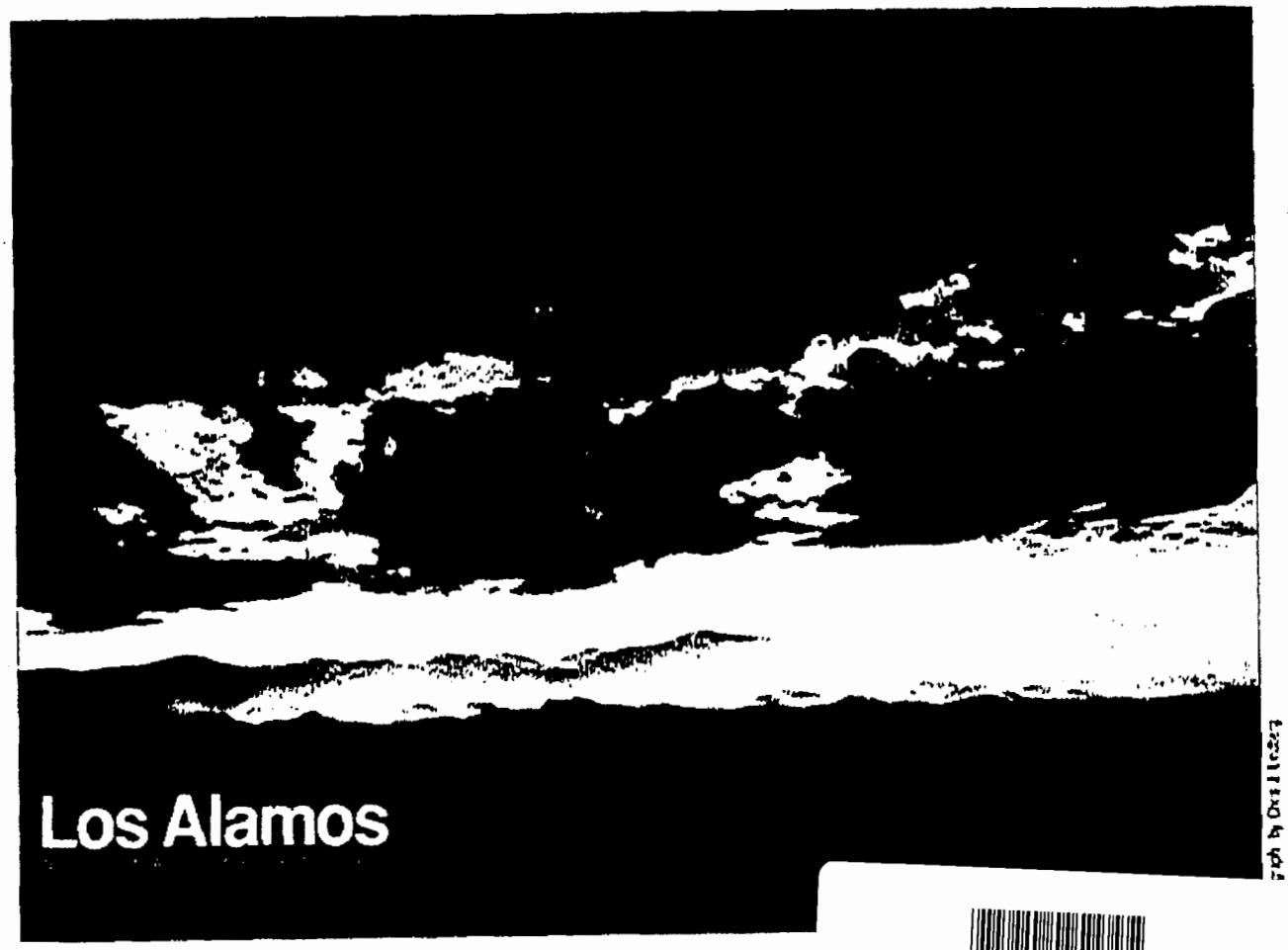

16401

LA-UR-96-1848 DRAFT I - 052296

DETERMINATION OF AN IN-SITU VADOSE ZONE VAPOR PHASE DIFFUSION COEFFICIENT AT A MESA TOP WASTE DISPOSAL FACILITY

Erik Vold[1] and Bart Eklund[2]
1. Los Alamos National Laboratory, Los Alamos, NM
2. RADIAN Corp., Austin, TX

Table of Contents

ABSTRACT....1
Introduction....2
Field Data....2
Moisture content and tritium concentrations in borehole samples....3
Permeability, in-situ vs. recovered core samples....3
Temporal variation of tritum flux and concentration in air....5
Tritium efflux from the ground surface....6
Analyses....7
Transport Equations....7
Vapor phase transport....8
Liquid phase transport....10
Combined phase transport....11
Numerical 3-D model....13
Numerical 1-D curvilinear model....16
Results....18
Tritium results, 3-D computations vs. field data....18
Tritium results, 1-D curvilinear computations vs. field data....19
Discussion....20
Best estimate of Deff from comparisons of field and model results....20
Determination of the in-situ vapor diffusion coefficient from Deff....22
Implications....23
Uncertainties....26
Conclusions....28
Nomenclature....29
Acknowledgment....29
References....30

Tables I and II....32
Figures 1 - 15....33

DETERMINATION OF AN IN-SITU VADOSE ZONE VAPOR PHASE DIFFUSION COEFFICIENT AT A MESA TOP WASTE DISPOSAL FACILITY

Erik Vold[1] and Bart Eklund[2]
1. Los Alamos National Laboratory, Los Alamos, NM
2. RADIAN Corp., Austin, TX

ABSTRACT

The Los Alamos National Laboratory Low Level Waste Disposal Facility, Area G, is located in a semi-arid region on the top of a narrow mesa composed of fractured layers of volcanic deposition known as Bandelier Tuff. Tritium, disposed in vertical shafts to depths of 60', has diffused by vapor transport through the mesa interior and from the mesa surface. Surface efflux measurements have characterized the scope of the tritium plume at the ground surface which gives a direct estimate of the in-situ diffusion scale length. Numerical and analytic diffusion solutions are compared to the field measurements to find an effective in-situ diffusion coefficient, D_{eff}, for tritium of $D_{eff} = 15 m^2/yr$. The diffusion coefficient estimates are consistent with a cylindrical source from the disposal shafts, implying tritium diffuses rapidly within the disposal shaft and then slower through the surrounding porous tuff. The tritium travels by combined vapor and liquid phase paths, dominated by vapor phase flow in the dry regime at Area G. In this situation, analysis indicates the observed effective diffusion coefficient corresponds to an in-situ vapor phase diffusion coefficient, D_{ins}, of $D_{ins} \sim 10^{-3}\ m^2/s$ within the mesa. This is about 40 times larger than that expected for vapor diffusion within the pore space of the Bandelier Tuff mesa. The data suggest the highly fractured volcanic tuff enhances the in-situ air permeability and convective flows driven by fluctuations in pressure or temperature further enhance the in-situ vapor diffusion or dispersion.

The relatively dry region observed in the immediate vicinity of the tritium plume suggests the vapor diffusion coefficient derived here will likely be conservative as a maximum value at Area G. Uncertainties suggest the result from this study is within a factor of two of the mean vadose zone vapor diffusion near the surface of the site. Analyses also suggest that the diffusion coefficient decreases below 60', and is smaller by about a factor of 4, than the value derived in this study. The in-situ diffusion enhanced by convective fluctuations implies that all gaseous species diffuse similarly, and thus the derived in-situ diffuson coefficient is a reasonable first estimate to apply in the assessment of transport of gaseous or vapor species other than tritium. The derived in-situ diffusion coefficient can also be used to quantify the water vapor flux and its significance relative to liquid phase transport in understanding the hydrology of the site.

Introduction

The observed distribution of tritium flux from the ground surface over an area where known quantities of tritium are disposed provides an opportunity to determine an effective in-situ vapor diffusion coefficient appropriate to the vadose or unsaturated zone beneath the mesa top low-level radioactive waste disposal facility at Los Alamos National Laboratory, Area G. This information is need for the Performance Assessment of the Area G disposal facilities [1] as required by USDOE orders. The results of this study are used to calibrate computational models and thus to accurately predict dispersion of vapor or gaseous phase contaminants from the disposal facility. The information also provides critical understanding of the basic hydrology at the site and can be used in quantifying the extent that vapor phase flow dominates within the mesa volume [2].

The disposal facilities at Area G are shown in Fig. 1 imposed on a contour map which shows the slope of the terrain. This highlights the edge of the irregular finger mesa with sides which fall abruptly about 100' (~30m) to the adjacent canyon floors. The saturated zone is estimated to be 900' (~270m) below the mesa surface, so that transport within the mesa and directly below occurs within the unsaturated or vadose zone. The upper layers of the mesa are highly fractured strata of volcanic deposition.

Tritium has been disposed in vertical shafts to 60' (20m) depth at the disposal facility for several decades. High-level tritium disposal occurs in the shaft field located in the central area within the highlighted box in Fig. 1, with the same area shown in detail in Fig. 2. Tritium efflux from the ground surface in the vicinity of the shafts has been accurately measured at the sample locations shown in Fig.2. This was previously reported in detail [3] and relevant field results will be summarized in this report.

The goals of this study are threefold: one, to compare field data with numerical and computational solutions to determine the best estimate of an 'effective diffusion coefficient' for the field observations of tritium, two, to use the analytic solutions for multiphase transport to derive an in-situ vapor diffusion coefficient from the effective tritium diffusion coefficient, and three, to examine relevant field data to determine how the diffusion estimate from the field measurements should be related to an average Area G value for gas or vapor diffusion within the mesa.

Field Data

The available field data of greatest importance in determining an effective scale length for the tritium diffusion from the disposal shafts are tritium ground surface efflux measurements. These allow one to 'map out' the surface area of the tritium plume and then to back calculate effective diffusion scale lengths for comparison to analytic and numerical solutions. These data are summarized at the end of this section. In order to better

interpret those surface flux measurements in terms of an effective diffusion coefficient, a number of relevant pieces of field data are presented first in this section. These data pieces will contribute to the discussion and interpretation of the results. In retaining the units associated with the original field data, some length scales are presented in units of feet, while some of the data and calculations are considered in metric units.

Moisture content and tritium concentrations in borehole samples

Moisture content and tritium concentrations in moisture from core samples recovered from two monitor holes drilled near the tritium disposal shafts are shown in Fig. 3 and 4. The locations of these monitor holes, NPH-8 and NPH-9, are shown in Fig. 1, with NPH-8 ~ 50' east of a high level disposal shaft, #154, and NPH-9 directly between two high level shafts, #150 and #151, separated from each other by less than 75'.

The moisture content (Fig. 3), determined by a calibrated neutron moisture probe [4], is especially low, about 1% volumetric, at depths of about 10 - 20m (30 - 60') in borehole NPH-8 and 5 - 22m (15 - 68') in NPH-9. This low moisture content region has been analyzed previously and found to be associated with negligible liquid phase flux [4] and a small vapor flux, typically ~ 0.1 cm/yr liquid equivalent flux [2]. The monitor hole, NPH-9, is the driest seen at Area G and the implied vapor flux there is the greatest seen at Area G. This vapor flux is locally ~ 1 cm/yr in magnitude (liquid equivalent flux) with no net flow direction apparent throughout the borehole or the dry region. The detected flux levels are comparable to the flux resolution, limited by the uncertainty of the analysis [2].

The tritium concentrations in moisture from recovered core samples are seen in Fig. 4. In both holes the tritium maxima are seen at about 20 m or about 60', the approximate maximum depth of the tritium disposal shafts. Both holes show an exponential decrease with greater depths, being very clear in the deeper hole, NPH-9, where the maximum tritium concentrations are found. At depths less than 20m or 60', the tritium concentrations decrease towards the surface in both holes, but there is a less distinct trend.

Permeability, in-situ vs. recovered core samples

Permeability measurements were made in a nearby borehole (NPH-5 or G-5) located as shown in Fig.1. This proximity is expected to give a reasonably good representation of profiles in the tritium shaft field region. In-situ air permeability was measured by a borehole packer isolation method using an air injection test method [5]. Independently, air permeability on core samples recovered from the same borehole was measured in the lab as a function of moisture content [6]. The air permeability values measured in the laboratory at the dry moisture content limit are shown in Fig. 5 and compared with the

in-situ permeability results verses depth in the borehole. The bottom figure shows the moisture profile for reference, and the stratigraphic unit interface locations. The three interfaces in this profile, using one of the standard nomenclatures (e.g., see Fig.3 in Ref.[7]), separate Units 2b, 2a, 1b, and 1a.

Both permeability values decrease with depth throughout the top unit (2b) to about 15m or about 50', with the in-situ value being about an order of magnitude larger at each location. In the second unit (2a) to depth 21m, the permeabilities approach a common value to within a factor of two. Below this there are local increases in both permeability values near the depth associated with a moisture spike at the 'vapor phase notch', ~ 23m. This depth is coincident with the interface between the devitrified and the vitrified tuff, and also near the elevation of an adjacent (Pajarito) canyon floor, which is saturated in portions of the canyon floor alluvium.

The in-situ permeability of 300 Darcies ($300.x10^{-12}m^2$) reported at 27m (~ 90') is a maximum limit of the measurement system [5]. It shows that the air injection test could not effectively isolate this interval either due to poor integrity of the borehole walls or the presence at this depth of a significant fracture traversing the interval. An interesting point and possibly significant correlation, is that the core sample recovered at 92' was also reported to have a fracture through the sample [6], which may have increased the permeability measured on the core sample as well. In either set of measurements then, the maximum permeability seen throughout the hole appears to coincide with the depth of the 'vapor phase notch'.

It is also noted that the horizon near the interface of Units 2b and 2a (~15m) does not exhibit unique values of permeability even though the moisture content decreases dramatically there. This supports the notion previously discussed [4] that this horizon is not unique in transport properties, but rather the depths above this are moister than usual due to proximity to moisture sources, either disposal units or fractures which conduct surface transients. Below 15m, the usual 'vapor phase dominated flow' exists [2] and is sufficient to create drying conditions which dominate the apparent moisture sources in the upper layer.

Air permeability differences between in-situ values and core samples similar to those observed here were first reported in detailed hydrologic studies [8] at Area G and Area L (adjacent to Area G) as summarized in [9]. They found the ratio of in-situ permeability, measured by the air-injection test method, to the laboratory analysis of core permeability to be factors of 16 to 22 in Units 2b and 2a, respectively, and factors of 4.6 and 3.3 in Units 1b and 1a, respectively. These values for the ratio of in-situ to core sample permeability, and the trend of a greater permeability ratio in Units 2 than in Units 1, is similar to that seen in Fig.5.

The larger permeability difference in Units 2 is consistent with observations of fractures on the walls of open disposal units which show a dramatic decrease in continuous fractures below the Unit 2b-2a interface. Previous observations throughout the local area have also shown a dramatic decrease in fractures continuing below the 'vapor phase notch' at the Units

1b-1a interface [10]. Atmospheric pressure fluctuations measured along the depth of isolated borehole segments have been observed to attenuate slowly to depths of about 100' and then more rapidly with greater depths [11]. This finding is consistent with a fracture network down to about 100' although there may be other explanations. This issue needs to be explored in future work.

Temporal variation of tritum flux and concentration in air

The temporal variation in tritium flux is not expected to significantly effect the observed scale lengths for the plume of tritium surface flux, and therefore it is not critical to the determination of the in-situ vadose zone diffusion coefficient. However, to better understand the tritum surface efflux, and to present a more complete set of field observations, several pieces of data on the temporal variability in tritium flux or airborne concentrations in atmospheric vapor are presented here.

A monthly averaged tritium surface flux was measured at a location in the east end of Area G over an older disposal unit in the early eighties [12]. Tritium flux data from that study verses month of the year is plotted in Fig. 6A, showing the seasonal variation over that particular interval and location. Monthly mean temperature data are also plotted in the figure and show a similar seasonal trend.

In the bottom figure (6B), the tritium flux is shown plotted against the mean monthly temperature values, and a linear regression is applied. With all the flux data points, the tritium flux, Γ_{H3} [Bq/m^2], is found to be linearly correlated to the ambient temperature, T_a [C], as

$$\Gamma_{H3}\,[Bq/m^2] = 0.336 - 0.172\,T_a\,[C] \qquad (1)$$

with a regression coefficient, r^2, equal to 0.59 indicating a modest correlation. By removing one point which appears in Fig.6B to be an outlier, the linear relationship is changed slightly, to

$$\Gamma_{H3}\,[Bq/m^2] = 0.345 - 0.140\,T_a\,[C] \qquad (2)$$

while the correlation coefficient improves to $r^2 = 0.81$, indicating a good correlation (~81% of the variance in flux is attributed to the temperature variation).

Tritium concentration in atmospheric moisture at two continuous air samplers located at Area G is shown in Fig. 7 for monthly averaged data collected over the period from 1984 to 1992. There is an apparent downward trend over the whole time, while the seasonal variation is also noted in most years. A large variability between the two stations and between different years is also apparent. These airborne tritium concentrations are well above the

regional background levels, typically less than 2 pCi/m^3 [13], and therefore are expected to correlate directly with the surface efflux from Area G.

As part of the detailed tritium surface flux study [3], surface flux measurements at one location were made over a 30 hour period to assess the diurnal cycle of tritium flux. The mass flux of moisture evaporated from the ground surface was measured at this location with results shown verses time of day in Fig.8. Also shown is several of the temperatures monitored as part of the flux study, the ambient air *(T-amb)*, the air temperature inside the tritium flux measurement chamber *(T-chamber)* described in the next section, and the soil temperature *(T-soil)* measured adjacent to the flux chamber location during the sampling.

The mass flux, as seen in the figure, varies by about a factor of four over the diurnal cycle, while the final results for tritum flux [3] varied in a similar pattern by a factor of 2.5 to 3. The tritium concentrations are not expected to change rapidly enough to see a diurnal variation, so the total moisture mass flux and the tritum flux should have similar values. The uncertainty in the moisture mass flux is smaller than the final uncertainty in the tritium flux numbers and so the mass flux in Fig.8 may reflect a more accurate portrayal of the diurnal variation of surface flux than the tritium numbers. Correlations to temperatures of the mass and tritum flux over this diurnal period were examined. The correlation with ambient temperature over this diurnal period resulted in a similar temperature dependence to that found above for the seasonal tritium flux variation.

Tritium efflux from the ground surface

Tritium flux from the ground surface was measured at over 300 points at Area G by RADIAN Corporation in an initial campaign during the summer of 1993 and in a followup study in 1994, with the complete results reported previously [3]. These flux measurements are made by an EPA approved sampling technique with extensive quality assurance. Each measurement samples a ground surface area of 0.13 m^2 and generally requires integration of surface flux over about a 4 hour period during the summer daytime conditions in order to collect an adequate moisture sample under the semi-arid conditions at the Area G site. The Area G flux study included measurements across all of Area G. For the present study, we will consider only the results from the area surrounding the high level tritium shafts at the sample locations that were identified in Fig. 2.

Following the first year of flux measurements, the tritium flux results were contoured on a facility map, as seen in Fig. 9, showing the *log of the tritium flux* in order to capture the full range of the results. This figure shows the sample locations from the first year (a subset of the complete locations shown in Fig. 2). The contours are generated by a simple interpolation scheme and show the area where the tritum plume falls to background levels. The results from all the sample points after the complete

two year sampling program did not change the contours greatly as will be discussed in the Results Section.

Analyses

Transport Equations

Comparison of the field results to model predictions requires an analytic framework for relating the transport of tritium via the vapor and liquid phases. The simple conceptual model for subsurface tritium migration is as follows. Tritium in the disposal shafts is assumed to oxidize rapidly in the near saturation conditions within the subsurface pore spaces and so it moves as tritiated water both in the vapor phase and in the liquid phase. Further reference to 'tritium' actually refers to tritiated water, indicated with the subscript, H_3. Tritium migration is assumed to be isotropic and at the ground surface, it is lost as evaporation.

In the vapor phase, tritium movement is driven by several mechanisms including pressure driven convective motion of the air through the pore spaces, diffusive vapor movement driven by gradients in moisture content and in temperature, and diffusive movement driven by the gradients in tritium vapor concentration. In the liquid phase, tritium moves with the subsurface water flow (unsaturated flow near Area G) and by diffusion in the liquid phase. The local tritium content will be dominated by the liquid phase, while the flux can have significant contributions from the vapor or the liquid phases depending upon the local conditions. Fluctuation driven vapor transport terms due to barometric or temperature oscillations may be important. They are included here in an empirical manner and will be elaborated in a separate forthcoming report. The following analysis which provides the framework for comparing model and field results is based on the work of Smiles et.al [14].

A single fluid continuity equation can be written,

$$\frac{\partial \rho}{\partial t} + \nabla \cdot \Gamma = 0, \qquad (3)$$

for mass density, ρ, and the flux, $\Gamma = \rho u$, which represents the bulk flow at average flow velocity, u. A multiphase approach is appropriate for transport via the parallel paths of vapor or liquid phase movement. Multiphase transport allows each species, i, to diffuse with respect to the bulk flow, described by the volumetric flux expressions given in the following discussion. This leads to a multiphase contiuity equation for species, i, in phase, j, of the general form

$$\frac{\partial(\theta_i \rho_i)}{\partial t} - \nabla \cdot \theta_i \rho_i u_i = \nabla \cdot (D_{ij} \nabla \rho_i) \tag{4}$$

where the phase volume fraction, θ_i, is folded into the effective diffusion coefficient, D_{ij}.

Phase volume fractions [phase volume/total volume] are indicated here as θ_a (for air including vapor) and θ (liquid phase). In media with porosity, η, then the relation, $\theta_a + \theta = \eta$, can be used to determine θ_a when η is known by measurements and θ is measured or computed. The vapor and liquid phase mass concentrations [mass/(phase volume)] for species, i, are denoted ρ_i and C_i, respectively. Diffusion occurs for the mass density, ρ_i, in the gas or vapor phase and occurs for a concentration, C_i, in the liquid phase, according to a diffusive flux,

$$\Gamma_{ia} = - D_{ia} \nabla \rho_i \tag{5}$$

for the air, gas, or vapor phase and

$$\Gamma_{iw} = - D_{iw} \nabla C_i \tag{6}$$

for the liquid phase, where the diffusion coefficient subscripts denote the species, i, diffusing through the media, air, a, or water, w).

The flux through a porous media is evaluated in terms of the empirically determined coefficients of permeability, k_p, hydraulic conductivity, K, (or unsaturated hydraulic conductivity as a function of water content, $K(\theta)$), and the matric potential, h_m (here expressed as a head in units of length). In the present study, the diffusion coefficients, D_{ia} and D_{iw} are also empirical.

Vapor phase transport

The volumetric convective flux for the air phase, q_a, is given as

$$q_a = \theta_a u_a = - \theta_a \frac{k_p}{\eta \mu_a} \nabla p, \tag{7}$$

where it is assumed that the permeability, k_p, has been evaluated for air in extreme dry conditions and therefore corresponds to transport through the full effective porosity, η, at air viscosity, μ_a.

In the case of water vapor as the species of concern, the vapor phase mass concentration depends strongly on temperature through the saturated vapor pressure and on the liquid phase moisture content as detailed

elsewhere [Refs.2,15,16]. In [2], it is shown that the vapor diffusion flux in air, Γ_{va}, can be rewritten approximately as

$$\Gamma_{va} = -D_{va}\nabla\rho_v = -D_{va}\,\rho_a\,\nabla\left(\frac{p_v}{p_s}\frac{p_s}{p_a}\right)$$

$$= -D_{va}\frac{\rho_a}{p_a}\left(\frac{dp_s}{dT}\nabla T + \frac{p_s}{h_c}\frac{dh_m}{d\theta}\nabla\theta\right) \qquad (8)$$

where p_s is the temperature dependent saturation vapor pressure, and h_c is the static equilibrium constant, $RT/(Mg)$, evaluated for the temperature and molar mass of the water vapor. The diffusion coefficient, D_{va}, is a net effective or in-situ diffusion coefficient in the pore space air. A weak dependence on absolute temperature is ignored in this approximation. Combining Eqn.7 with Eqn.8, the total vapor flux, Γ_v, includes the contribution from the convective air movement, q_a, carrying vapor density, ρ_v, and the vapor diffusion contribution, or

$$\Gamma_v = -\rho_v\,\theta_a\frac{k_r}{\varepsilon\mu_a}\nabla p - D_{va}\frac{\rho_a}{p_a}\left(\frac{dp_s}{dT}\nabla T + \frac{p_s}{h_c}\frac{dh_m}{d\theta}\nabla\theta\right) \qquad (9)$$

For the case of tritiated water movement, in addition to this vapor gradient driven diffusive flux, there is also a diffusion flux driven by the gradient in tritiated water vapor, $\rho_{H3:v}$. The net flux of tritiated water in the vapor phase, $\Gamma_{H3:v}$, then becomes,

$$\Gamma_{H3:v} = \rho_{H3:v}\,q_v - D_{va}\,\nabla\rho_{H3:v} \qquad (10)$$

where $q_v = \Gamma_v/\rho_v$ and Γ_v is given above in Eqn.9. The net effective diffusion coefficient, D_{va}, observed for vapor or tritium transport in the field can result from several possible mechanisms as discussed in the following.

The pressure gradient and temperature gradient terms in Eqn.9 are oscillatory in the subsurface environment and are expected to decay with depth from the surface where periodic forces cause the barometric pressure and the temperature to vary with daily and seasonal fluctuations. These terms drive oscillatory convective motion which can enhance the effective in-situ diffusion coefficient, D_{va}. In fact, the pressure oscillations can enhance the temperature gradient diffusion coefficient which will then increase the temperature gradient flux. This can in turn enhance the effective diffusion coefficient in the moisture gradient and in the tritium concentration gradient terms. The nature of these oscillatory forces and the resulting transport is planned to be analyzed in a subsequent and separate report.

For our purposes here, it is sufficient to note that there are several possible driving terms which can enhance the observed diffusion coefficient

above that expected for static diffusion into the air. Philips and deVries [15] reviewed several experimental studies where it was seen that the effective diffusion was 4 to 20 times greater than the simple theory (classical diffusion into still air in a porous media) and they investigated the temperature dependent term as the possible cause.

Barometric pumping has been suggested as a significant mechanism in the Los Alamos mesa subsurface environment by several investigators. In a recent preliminary estimate, the contribution to the effective diffusion at Area G due to naturally occuring barometric pumping was quantified and found to be a possible cause of the observed effective diffusion [17]. That estimate will be considered further in the Discussion section. In-situ air permeability was seen in the previous section to be an order of magnitude larger than the core sample air permeability at many horizons under Area G. Surface connected fractures, or subsurface areas disturbed by disposal excavations are assumed to contribute to the increased in-situ permeability. This is likely to enhance effective diffusion and may have a combined effect with the mechanisms which can drive oscillatory flow through the regions of increased permeability.

Returning to our present purpose, there is likely to be an effective diffusion coefficient at play in the in-situ environment which is enhanced above that expected by the simple theory of isothermal diffusion into static air in a porous media. It is the total effective diffusion coefficient, D_v, we are to determine in comparing model results to field studies of tritium diffusion.

The vapor flux was found to be small at Area G in the boreholes in the vicinity of the tritium disposal shafts [2]. That result assumed a large effective diffusion coefficient based on preliminary estimates from this present study, and is likely to be a maximum estimate of the actual vapor flux. Because the gradients will be dominated by the gradient in tritium concentration, then it is safe to assume the following conditions apply. The tritium vapor flux in the region near the tritium disposal shafts is dominated by the tritium gradient driven diffusion term, which is characterized with an effective or in-situ diffusion coefficient. The background flux of vapor due to gradients in pressure, temperature, or moisture content will be much smaller under the conditions at Area G.

Liquid phase transport

The volumetric flux for the liquid phase or Darcy flux, q, can be written for the unsaturated zone in the form

$$q = \theta u = -K \nabla h = -K \nabla(h_m + z), \qquad (11)$$

in terms of the empirically determined parameters, unsaturated hydraulic conductivity, $K[\theta]$ and the moisture matric potential or tension, $h_m[\theta]$, expressed as a head in units of length.

The liquid phase flux of tritiated water, $\Gamma_{H3,w}$ in the unsaturated subsurface comes from combining Eqns.11 times the tritium liquid concentration, $C_{H3,w}$, with Eqn.6 to obtain

$$\Gamma_{H3,w} = C_{H3,w}\, q - D_{H3,w} \nabla C_{H3,w} . \qquad (12)$$

The unsaturated hydraulic conductivity, $K(\theta)$, which drives convective liquid phase flow, q, as in Eqn.11, decreases exponentially as moisture content decreases. In the very dry conditions prevailing at the tritium disposal site (as seen in Fig.3), it was determined that the Darcy flux in the boreholes, NPH-8 and NPH-9 was negligible throughout much of the profile [4]. It is safe to assume that the Darcy flux, q, is negligible compared to the liquid phase diffusive flux term in the region near the tritium disposal at Area G.

Combined phase transport

The vapor phase continuity equation for tritum with decay constant, λ_{H3}, in a source free region becomes

$$\frac{\partial(\theta_a \rho_{H3,v})}{\partial t} + \nabla\cdot(\rho_{H3,v}\, \Gamma_v) = \nabla\cdot(D_{va}\, \nabla \rho_{H3,v}) - \lambda_{H3}\theta_a \rho_{H3,v} . \qquad (13)$$

The liquid phase continuity equation for tritum becomes

$$\frac{\partial(\theta\, C_{H3,w})}{\partial t} + \nabla\cdot(C_{H3,w}\, q) = \nabla\cdot(D_{H3,w}\, \nabla C_{H3,w}) - \lambda_{H3}\theta\, C_{H3,w} . \qquad (14)$$

The tritium vapor and liquid concentrations are partitioned in the same way as are the water vapor and liquid water at the same temperature, and are thus related as the ratio of their densities and in terms of pressures as

$$\frac{\rho_{H3,v}}{C_{H3,w}} = \frac{\rho_v}{\rho_w} = \frac{p_v \rho_s \rho_a}{\rho_s p_a \rho_w} \sim \frac{p_s \rho_s \rho_a}{\rho_s p_a \rho_w} \sim \frac{p_s \rho_a}{p_a \rho_w} \equiv H, \qquad (15)$$

using the saturation (subscript s) values for density and pressure, and noting that $p_v \sim p_s$. This expression defines the ratio, H, (the same H as used by Smiles,et.al.[14]). It is evaluated at a seasonal average temperature of $T = 10^o$ C, using $p_s/p_a \sim 13mbar/1000mbar$ [Ref.2] and $\rho_a/\rho_w \sim 1.2 \times 10^{-3}$, so that $H = 1.56 \times 10^{-5}$. Expressing the vapor concentration as $\rho_{H3,v} = H\, C_{H3,w}$, from Eqn.15, the total tritium is therefore approximately equal to that in the liquid phase,

$$\theta_a \rho_{H3,v} + \theta\, C_{H3,w} = (1 + (\theta_a/\theta)\, H)\, \theta\, C_{H3,w} \sim \theta\, C_{H3,w} . \qquad (16)$$

The vapor phase and liquid phase continuity equations for tritum are next added together to yield a combined phase or total tritium continuity equation which can be written,

$$\frac{\partial(\theta C_{H3,w})}{\partial t} + \nabla\cdot(C_{H3,w}\, q + \rho_{H3,v}\, \Gamma_v) =$$

$$\nabla\cdot(D_{H3,w}\, \nabla C_{H3,w} + D_{vn}\, \nabla \rho_{H3,v}) - \lambda_{H3}\theta\, C_{H3,w} \qquad (17)$$

As described above, in the conditions that prevail at Area G, it is a good assumption to neglect the convective flux for the vapor, Γ_v, and for the liquid, q, relative to the tritium gradient driven diffusive flux. Although these convective fluxes are negligible, the fluctuation convective mechanisms may still act to enhance the effective tritium vapor diffusion coefficient, D_{vn}. This simplifies the tritium continuity equation, effective at Area G conditions, to

$$\frac{\partial(\theta C_{H3,w})}{\partial t} = \nabla\cdot(D_{H3,w}\, \nabla C_{H3,w} + D_{vn}\, \nabla \rho_{H3,v}) - \lambda_{H3}\theta\, C_{H3,w}$$

$$= \nabla\cdot((D_{H3,w} + H\, D_{H3,v})\, \nabla C_{H3,w}) - \lambda_{H3}\theta\, C_{H3,w} \qquad (18)$$

Under the assumptions, one, that moisture is a slowly varying function of time (demonstrated to be valid for vapor and for liquid phase transport, respectively in Refs.[2] and [4]), and two, that the diffusion coefficient is approximately constant in space, (or if a spatially averaged value is assumed) then this becomes

$$\frac{\partial(C_{H3,w})}{\partial t} = \frac{(D_{H3,w} + H\, D_{vn})}{\theta}\, \nabla\cdot(\nabla C_{H3,w}) - \lambda_{H3}\, C_{H3,w}$$

$$= D_{eff}\, \nabla^2 C_{H3,w} - \lambda_{H3}\, C_{H3,w} \qquad (19)$$

where this defines an 'effective diffusion coefficient' with respect to liquid phase concentration of tritium, which is migrating in the field by vapor and liquid phase diffusion. The vapor diffusion is in turn possibly enhanced due to oscillation effects, dual permeability interactions, or other unknown effects.

Under the semi-arid conditions assumed by Smiles et.al. [14], the liquid phase diffusion will be small compared to the vapor phase diffusion at moisture contents below about 20%, and it will decrease with moisture as $\theta^{H/3}$. The Area G tritium study area is well below the 20%, averaging about 1% volumetric throughout the region near the tritium waste sources. It is a good assumption in these conditions to simplify the above expression further

by neglecting liquid phase diffusion and redefining the effective diffusion coefficient at Area C, as

$$D_{eff}\,(Area\ C) \sim \frac{H\,D_{va}}{\theta}\ . \tag{20}$$

As used here, the tritium vapor diffusion coefficent, D_{va}, incorporates corrections to account for the porous media and for unknowns in the realistic field conditions. It is convenient to account for these effects in two separate factors, $\varepsilon_a(\theta_a)$ and A_D, such that

$$D_{va} = \varepsilon_a(\theta_a)\,A_D\,D_{bda} \tag{21}$$

where D_{bda} is the binary diffusion coefficient for water vapor diffusing in air. The factor, $\varepsilon_a(\theta_a)$ is less than one, and accounts for porosity, tortuousity and the actual air volume fraction. Millington [18] originally suggested the dependence used by Smiles et.al.[14], that $\varepsilon_a(\theta_a) \sim \theta_a^{4/3}$. The combination, $(\varepsilon_a(\theta_a)\,D_{bda})$, is the diffusion within the pore space expected by 'classical theory in a porous media' as described by Philips and deVries [15].

The factor, A_D, is considered a 'diffusion amplication factor' equal to the in-situ diffusion relative to the classical diffusion. The 'in-situ vapor diffusion' is actually a vapor dispersion which accounts for any empirical factors that act to enhance the in-situ diffusion, including barometric or temperature oscillation driven flux, coupling to a second media with different permeability (e.g., a fracture network), or other unspecified effects. An in-situ diffusion coefficient, D_{ins}, is defined as

$$D_{ins} = A_D\,D_{w,a}. \tag{22}$$

This assumes that the porous media correction is made in $\varepsilon_a(\theta_a)$ and then D_{ins} represents the in-situ diffusion within the pore space due to enhancements over classical diffusion. With this in-situ value, a comparison to the classical binary diffusion coefficient provides a direct estimate of the in-situ enhancement, or diffusion amplification factor, A_D.

The equations developed in this section will be used in the interpretation of the results.

Numerical 3-D model

For numerical modeling, it is convenient to write a general equation governing the production, decay and diffusive transport of a nuclide's concentration, C_i, (similar to Eqn.19) as

$$\frac{\partial C_i}{\partial t} + \lambda_i C_i - \nabla(- D_{i,eff} \nabla C_i) = S_i \qquad (23)$$

where λ_i is the radiologic decay constant for nuclide, i, $D_{i,eff}$ is the effective diffusion coefficient for nuclide i through the combined transport paths in the matrix and S_i is a source of nuclide i. In our case, the source represents diffusion from the waste package, and is a continuous source. This can be specified using a volumetric source term as in Eqn.23 and as described below for the numerical implementation. The continuous source can also be specified as a flux boundary condition in attempting to derive an analytic solution to the 1-D problem.

A point source of negligible volume and an initial concentration of tritium, C_0, was treated by Smiles, et.al.[14] where the analytic solution is found to be of a general form,

$$C_i \propto C_0 (D_{i,eff}\, t)^{-3/2} \exp(- r^2/(4 D_{i,eff}\, t) - \lambda t). \qquad (24)$$

The scale length, L_a, for the exponential attenuation expected in the field due to diffusion is seen from the exponential arguement to be $L_a = \sqrt{4\, D_{i,eff}\, t}$. In this case, the part of the solution due to the decay of tritium, $exp(- \lambda t)$, is separable because all tritium is introduced at a single time, $t = 0$. However, in the case of a constant source needed to represent the continuous loss of tritium from a waste package, then the decay correction is less straightforward, and the analytic solution must be integrated in time and in the appropriate geometry.

Analytic solutions for the case of the continuous source of a conservative (non-decaying) species in spherical geometry are expressed in terms of the complimentary error function, while the solution in cylindrical geometry is expressed in terms of the exponential integral (see for example, sections 10.2-10.3 in Ref.[19]). The solution to the continuous source in planar geometry combines an exponential term, as in Eqn.24 above, with a term involving the complimentary error function. In each of these cases, the characteristic scale length in the arguement of the integral function is the same,

$$L_a = \sqrt{4\, D_{i,eff}\, t}\,. \qquad (25)$$

This will prove useful for scaling results at a given time, independent of the geometry, using diffusion coefficients, D, and scale lengths, L, as

$$\left(\frac{D_1}{D_2}\right) = \left(\frac{L_1}{L_2}\right)^2. \qquad (26)$$

The complexity of the analytic solutions in the actual case of a continuous source with species decay and in spherical or cylindrical

geometries, led us to the approach where the governing diffusive equation [23] is solved numerically. This was done for two cases. In one, a 3-D rectilinear grid is used with sources located at estimated depths, based on actual inventory, and a uniform diffusion coefficient is used. In the second case, the decayed diffusive transport equation is solved numerically in a 1-D curvilinear geometry which can be modified to represent either cylindrical or spherical geometry.

The diffusion equation [23] for a constant diffusion coefficient, D, in 3-D rectilinear coordinates is

$$\frac{\partial C}{\partial t} + \lambda C = D\left(\frac{\partial^2 C}{\partial x^2} + \frac{\partial^2 C}{\partial y^2} + \frac{\partial^2 C}{\partial z^2}\right) + \frac{C_{in}(x,t)}{\tau} . \qquad (27)$$

A computational model implements this form with empirical coefficients chosen to match tritium surface efflux measurments. These coefficients include a constant diffusion coefficient, D, a shaft-specific release time constant, τ, and a shaft-specific source concentration, $C_{in}(x,t)$. This latter factor is evaluated as a delta function, non-zero only at the locations of the waste disposed within the high level shafts.

The magnitude of the tritium plume depends upon the source concentration and release rate while the characteristic dimensions, or spatial attenuation length, of the plume will depend only upon the effective diffusion coefficient (as in Eqn.25) in the subsurface media for a given source geometry and known decay constant, λ. Therefore, an attenuation length observed for the tritium plume in the field can be used to assess the effective diffusion coefficient. If desired, the tritium concentrations in core moisture can be used to estimate the release rate, τ, when the source quantities, $C_{in}(x,t)$, are known. A detailed evaluation of the value for τ is beyond the scope of this study, but a preliminary estimate is given in the Discussion section.

The computational volume was specified with the number of grid points per axis as, $nx = 30$, $ny = 40$, $nz = 20$ and with grid spacing dimensions as $dx = 20ft$, $dy = 20ft$, $dz = 7.5ft$ in the initial runs. Some final runs used a finer resolution, $dx = dy = 10\ ft$, to resolve the attenuation length around the shafts. The numerical code integrates the transport operators explicitly in time and treats the radiologic decay term implicitly using standard difference approximations [e.g., see Ref.20]. The top computational surface corresponds to the ground level. Tritium flux to this boundary is assumed lost to the atmosphere. The other boundaries are far enough from the source that the boundary conditions there have a small impact on the solution.

The source data input to the 3-D model is summarized in Table I. The source concentrations of tritium, $C_{in}(x,t)$, are specified by year and by 3-D location for the model input as

$$C_{w0}(x,t) = C_{w0}(x,y,z, t > t_i) \exp(-\lambda(t-t_i)) \quad (28)$$

for each of the 10 maximum annual shaft disposals entered in the Area G inventory data base, where t_i is the time of disposal of tritium quantity, A_0, and the source concentration, C_{w0}, is simply taken as the annual disposal quantity, A_0, divided by the local grid cell volume. These 10 disposals cover more than 95% of the tritium disposed at Area G, and happen to occur in only three shafts with the greatest inventory, #150, #151 and #154. The operating life times for each of the disposal shafts are used to approximate the depth, z, for tritium disposal in each year, assuming a linear filling of the disposal shaft over its lifetime. The values for shaft release time constants, τ, were chosen to best match the field results. The value for τ at the newer steel lined shaft #154 was initially taken to be 5 times larger than the value at the older unlined shafts, #150 and #151. This seemed to match the preliminary field data best in a qualitative manner, however, in the final analysis, it was seen that the shafts all had similar release rates and the same value of τ was used to characterize the release from each of the shafts.

The 3-D model simulation is run explicitly from the time of the oldest tritium disposal to the date of the field study for comparison to field data. The results are discussed in a following section.

Numerical 1-D curvilinear model

The geometry of the tritium source (see Fig.10) and subsequent diffusion problem can be characterized in spherical geometry or in cylindrical geometry depending upon the diffusive characteristics of the soil matrix relative to that of the disposal shaft itself. Both geometries are considered here and the results and implications compared in the Discussion section. First, spherical geometry is assumed with isotropic diffusion from a point source at the tritium waste package location. This neglects the differences in diffusion characteristics through the tuff matrix and through the disposal shaft volume. Second, a cylindrical geometry is assumed, consistent with a tritium source diffusing rapidly throughout the disposal shaft volume relative to its slower diffusion in the tuff matrix.

The waste sources containing tritium were seen in Table I to be dominated by a few waste packages disposed at specific times and therefore related to specific depths within the disposal shafts. This could be modeled in spherical geometry for each tritium source at each disposal depth. To simplify this case further, the tritium waste is approximated as being located in a single waste package in each shaft at a single 'effective' disposal depth. This 'effective depth' for each shaft is listed in Table II, labeled as d_{eff} -ft-, where this value is estimated from the actual disposal quantities and depths indicated in Table I. The disposal shaft geometry used for the spherical geometry approximation is sketched in Fig. 10.

In this Figure 10, the tritium plume observed at the surface has an exponential decay length on the ground surface of L_g. This plume surface dimension is determined from the contours of the field data results by measuring the e-folding distance around each shaft in each of the four cardinal directions. The average and deviation of these four lengths are shown in Table II, labeled as L_g for each of the shafts, with the average across the three shafts of L_g = 27.7*ft* with an 18% variation between shafts. It is an approximation that the e-folding length is taken as the appropriate attenuation length, independent of the geometry.

For isotropic diffusion from a point source where the geometry and cross-section of the disposal shaft itself are neglected, then the tritium concentration at point A (Fig.10) is the same as at the point, D, equidistant from the assumed single-point source at point, C. Thus, the attenuation length of L_g observed along the surface corresponds to the attenuation length of L_{sp}, projected along the spherical axis of symmetry centered at the waste source, C. It is evident from the figure that the length, L_{sp} is given as

$$L_{sp} = \sqrt{d_{eff}^2 + L_g^2} - d_{eff} . \qquad (29)$$

This value, L_{sp}, is determined from the surface attenuation lengths observed for the field data, L_g, and from the assumed effective depth, d_{eff}, to the point source for each shaft in Table II. The average value over the three shafts is L_{sp} = 10.6 *ft*. This attenuation length corresponds to the observed field conditions if the source is diffusing with spherical symmetry.

If tritium migrates rapidly within the volume of the disposal shaft relative to its migration through the tuff matrix surrounding the shaft, then the effective geometry for the tritium source for diffusion into the tuff would be cylindrical. As the source geometry approaches a cylinder, then d_{eff} in Fig.10 goes to zero and so the projected scale length, L_{sp}, approaches the scale length observed at the surface, L_g. This point will be used to show the results are more consistent with a cylindrical source geometry than with the spherical source geometry assumed initially in the numerical modeling.

To compare results in both geometries, the tritium diffusion problem was examined in the spherical and in the cylindrical case. As discussed above, an analytic solution was not determined for the actual field conditions which incorporates a flux boundary condition appropriate to the long term release from the disposal waste package. Therefore, the 1-D tritium diffusion equation was solved numerically in the two geometries.

The numerical problem was treated by finite differencing the diffusion operator, $\nabla(D\nabla C)$ from Eqn.23, for 1-D geometry using a constant grid size, Δr, with index, i, along the 1-D axis, as

$$\nabla(D\nabla C) = \frac{1}{\Delta r(i)^2\, cc(i)} \times$$

$$\left(\left(\frac{(cc(i) + cc(i+1))}{(1/D(i) + 1/D(i+1))} \right) \left(C(i+1) - C(i) \right) - \left(\frac{(cc(i) + cc(i-1))}{(1/D(i) + 1/D(i-1))} \right) \left(C(i) - C(i-1) \right) \right). \tag{30}$$

The geometry factor, $cc(i)$, can be modified to accomodate the desired geometry, $cc(i) = r(i)^2$ for spherical geometry, $cc(i) = r(i)$ for cylindrical geometry, and $cc(i) = 1$ for planar geometry. This expression can also accomodate a spatially varying diffusion coefficient, $D(i)$, but this option was not exercised in the present study. Results in the spherical and cylindrical geometries are presented in the following.

Results

Tritium results, 3-D computations vs. field data

In preliminary calculations of the tritium diffusion in the 3-D model a diffusion coefficient of 100ft^2/yr (~10m^2/yr) was found to be qualitatively in good agreement with the early field results shown in Fig.9 [Ref.17]. The tritium results from the 3-D model are shown in Fig.11 for comparison. Computational results show in-situ concentrations (log of concentration data), which are directly comparable to the surface flux measured in the field data, provided that the evaporation rate is reasonably constant throughout the surface area. This is a reasonable assumption for the field conditions where vegetative cover is consistently sparse in the vicinity of the tritium disposal shafts.

The top of the computational volume in Fig.11 corresponds to the ground surface, and it can be seen that the sources introduced into the three high level shafts provides a qualitatively good match to the field data in Fig.9. Figure 11 also shows some isomeric surfaces of concentration levels which reveal the higher tritium concentrations in the subsurface vicinity of the disposal shafts. It shows that at the highest concentration levels depicted, only two shafts (#150, and #151) contribute in this simulation.

In Fig.12, the computed tritium results (log concentrations) for the surface plane are extracted from the 3-D solution and shown, comparing 3 values of the diffusion coefficient, $D = 50\ ft^2/yr$, $D = 100\ ft^2/yr$, and $D = 250\ ft^2/yr$. Considering the scale of these figures it appears qualitatively that the best agreement with the field data is for the results in the range, $D = 50 - 100\ ft^2/yr$.

The results in Figs. 9, 11 and 12 depict the log of the tritium concentration (or flux) values, where the log transform is important to

visualize the range observed in the tritum data. However, the contour plot of the log of the data is sensitive to the background level and to the magnitude of the source above the background. Because the diffusion solution is exponential, the log of the solution will decay linearly with distance from the source and only levels out at the background concentration. Thus, the log contour plots are sensitive to the source strength and to background levels and are not convenient to quantify an e-folding or attenuation length. Rather, they provide a good estimate of the scale length over which the solution falls to the level of the background concentration.

To avoid this problem, the solutions for the field observations and from the 3-D model were replotted in linear scales to more accurately determine an e-folding attenuation length to represent the characteristic diffusion scale length. The contour results of the (linear) tritium field flux data are shown in Fig.13 with an inset that compares contours from the 3-D solution using a constant diffusion coefficient of $D_e = 150\ ft^2/yr$. Note that the inset area (for computed results) is approximately equivalent to the dashed area for the field results, but the contour levels are not quantitatively comparable between the field and computed results. The computed results were plotted with several different contouring levels to best resolve the attenuation around each of the shafts. From these plots, the surface attenuation (1/e) scale length for the 3-D calculation, L_{ge}, was determined from four different plume transects, and found to be $L_{ge} \sim 20' \pm 5'$.

This can be compared to the value for the ground surface scale length determined from the observations, $L_g = 27.7' \sim 28'$ in Table II, an average from around the three shafts of concern. Using these results with the scaling law, Eqn.26, the diffusion coefficient in the 3-D model calculation that would reproduce the scale length observed in the field data is $D_{3D}(L_{ge} = L_g)$, where

$$D_{3D}(L_{ge} = L_e) = D_e \left(\frac{L_g}{L_{ge}}\right)^2$$
$$= 150\ ft^2/yr \left(\frac{27.7}{20}\right)^2 \sim 290\ ft^2/yr \sim 27\ m^2/yr. \tag{31}$$

This is a first estimate of the effective diffusion coefficient from the 3-D model compared to the field data.

Tritium results, 1-D curvilinear computations vs. field data

Results from the 1-D model for a point source in spherical geometry are compared for two diffusion coefficient values, $D = 100\ ft^2/yr$ and $D = 200\ ft^2/yr$ in Fig.14. From the figure, the attenuation length is seen to be constant in the intermediate range of distances, where the grid resolution near the source and the far boundary condition do not influence the diffusion. From the figure, the observed attenuation lengths over these intermediate distances

for the two cases are $L_s(D=100ft^2/yr) \sim 17'$ and $L_s(D=200ft^2/yr) \sim 24'$. Their ratio, $L_s(D=200ft^2/yr)/L_s(D=100ft^2/yr) = 24/17 \sim 1.4 = \sqrt{2}$, as expected from the analytic solution scaling law, Eqn.26, for $D_1/D_2 = 200/100$.

Again, the scaling law is used to estimate the diffusion coefficient needed in the numerical computation to match the observed field results. The scale length for a point source in spherical geometry projected from surface attenuation length observations, L_0, was denoted, L_{sp}. This was determined using Fig.10 and Eqn.29, resulting in $L_{sp} = 10.6ft \sim 11ft$ as summarized in Table II. Using the scaling Eqn.26, the diffusion coefficient in the 1-D spherical numerical solution which will match this field observed value is $D_{1Ds}(L_{sp} = L_s)$, evaluated as

$$D_{1Ds}(L_{sp} = L_s) = 100ft^2/yr\left(\frac{11}{17}\right)^2 = 42\ ft^2/yr \sim 4\ m^2/yr. \qquad (32)$$

This estimate will be compared in the Discussion to the previous value from the 3-D model results of $27m^2/yr$.

In Figure 15, the diffusion solution is evaluated for a diffusion coefficient of $D=150ft^2/yr$, and compared for the cases of spherical (point source) and cylindrical (line source) geometry. The observed attenuation lengths from that figure respectively for the spherical and cylindrical case, are $L_s\ (D=150ft^2/yr) \sim 21'$ and $L_c\ (D=150ft^2/yr) \sim 25'$. This spherical case result is consistent with the cases shown in the previous figure and with the scaling law, Eqn.26.

If the whole vertical disposal shaft acts as the tritium source term, and if one can neglect 'end effects' near the ground surface, then release of tritium can be approximated in cylindrical geometry. In this case, the cylindrical solution in Fig.15 can be corrected to the observed field attenuation lengths, to provide an estimate of the diffusion coefficient if the source is cylindrical. The field scale length to use in this case is $L_0 = 27.7\ ft$ from Table II, and so the corrected diffusion coefficient estimate for a cylindrical source geometry, D_{1Dc}, becomes

$$D_{1Dc}(L_c = L_0) = 150ft^2/yr\left(\frac{27.7}{25}\right)^2 = 184\ ft^2/yr \sim 17\ m^2/yr. \qquad (33)$$

Discussion

Best estimate of D_{eff} from comparisons of field and model results

The disposal shaft is backfilled with crushed tuff. Crushed and intact tuff have similar transport properties, so it is not obvious which geometry,

spherical or cylindrical, should be the more accurate case. If the shafts are tightly packed after being backfilled, a spherical source geometry may exist, while if the disposal shafts are less tightly packed, then a cylindrical source is likely, as the tritium diffuses rapidly throughout the shaft before diffusing significantly into the surrounding tuff.

Comparisons of numerical calculations in 'spherical geometry' with field results provided disparate estimates of the effective diffusion coefficient, $27 m^2/yr$ using the 3-D model and $4\ m^2/yr$ using the spherical geometry 1-D model. (The 3-D model is effectively in spherical geometry because it specifies a set of point sources which have been located at a few discreet point locations within the disposal shafts and the diffusion is isotropic.) A simple average of these estimates is $15.5 m^2/yr$. A geometric mean of the two estimates is $10\ m^2/yr$ with geometric standard deviation of almost 4, indicating a large discrepency.

The first two numerical models (3-D and 1-D spherical) differ in the way spherical geometry is incorporated. In each case, if the source term were in cylindrical geometry, the diffusion coefficient estimate needed to match field data would tend to converge towards some intermediate value of the estimates in spherical geometry. This was shown directly in Eqn.33 for the 1-D cylindrical geometry case where the diffusion coefficient becomes $17\ m^2/yr$.

In the 3-D numerical case, the sources were input at discreet depths (Table I) and the uniform diffusion coefficient assumption does not distinquish any different properties of the disposal shaft itself. Thus, the effective depth is approximately the actual disposal depth. If diffusion were rapid within the disposal shaft relative to that through the tuff matrix surrounding the disposal shaft, then the source would be effectively cylindrical and the 'effective depth' to the source would be less than the depth to the actual tritium waste packages. Refering to Fig. 10, an effective depth can be calculated which allows the computed scale lengths to match the observed scale lengths. For the case with $D=150 ft^2/yr$, this occurs for depth, ~ 30ft. This is a reasonable estimate for the effective depth in cylindrical geometry. This is slightly less than the waste depths assumed (Table I) and shows the strong sensitivity of the results to the assumed effective depth.

These considerations support an estimate of the diffusion coefficient near the value used in the simulations shown in Fig.11 of $D=150 ft^2/yr$ $(14 m^2/yr)$. The uncertainty in the source term geometry, especially in the 3-D simulations, leads to a large uncertainty in the final estimate of the diffusion coefficient in this method as discussed later.

Additional 3-D simulations were run with the source modeled as a cylinder which did show good agreement between the 3-D model and field results when the top of the cylinder was located below the depth of 20' (3 grid cells from the surface). The implications of the field data and computational comparisons are clear that the source term is effectively cylindrical. The 3-D code would need to be modified to allow different diffusion characteristics inside the disposal shaft compared to outside the shafts, in order to more

realistically match the field data. The 3-D code results cannot provide an accurate match to field results with the constant diffusion coefficient used in the present study.

Tritum flux values measured directly over the disposal shaft caps were high as discussed in detail previously [3], and were not included in the contour results for the field data in Fig.9 or in Fig.13. It was calculated [3] that about 90% of the tritium flux was emitted from the shaft cap circumference. Only 10% of the total tritium is depicted in Fig.9, diffusing through the soil or tuff matrix. This supports the finding that the source geometry is effectively cylindrical, coinciding with the disposal shaft geometry, and confirms the implication that the tritium released from the waste packages diffuses relatively rapidly throughout the disposal shaft and then slower from the shaft through the surrounding tuff.

Summarizing the model and field data comparisons, the average of the initial estimates from the two numerical methods in comparison to field observations and assuming spherical geometry was 16 m^2/yr, and using the 1-D cylindrical geometry, a diffusion coefficient of 17 m^2/yr was estimated. In the 3-D code, $D = 14\ m^2/yr$ was used in simulations which matched the field results if the 'effective depth' of a cylindrical source were reduced to about 30' or less. The combination of these estimates suggests that the effective diffusion coefficient is about $15 m^2/yr$. The following analysis assumes this value applies to this region of Area G, and so the effective in-field tritium diffusion coefficient is taken to be

$$D_{eff}\,(Area\ G) \sim 15 m^2/yr. \tag{34}$$

Determination of the in-situ vapor diffusion coefficient from D_{eff}

Combining Eqns.20 and 21, the effective diffusion coefficient for tritiated water, D_{eff}, is related to an insitu gas or vapor phase diffusion coefficient, D_{ins}, defined in Eqn.22, as

$$D_{eff}\,(Area\ G) \sim \frac{H\,D_{va}}{\theta} \sim \frac{H\,\varepsilon_a(\theta_a)\,D_{ins}}{\theta}. \tag{35}$$

We assume the form for $\varepsilon_a(\theta_a)$ used by Smiles et.al.[14], based on work by Millington [18], that $\varepsilon_a(\theta_a) \sim \theta_a^{4/3}$. From the vertical profiles of moisture near the tritium shafts (Fig.3) the average moisture content in the vicinity is about $\theta \sim 0.01$. The average porosity for units 2b and 2a which surround the tritium disposal shafts are very nearly equal to 0.47 [Ref.21]. Thus, in the vicinity of this study, θ_a is approximately equal to $0.47 - 0.01 = 0.46$. This gives the porosity correction at the disposal shafts vicinity of

$$\varepsilon_a(\theta_a) \sim 0.46^{4/3} \sim 0.36. \tag{36}$$

The in-situ diffusion coefficient for vapor phase transport in this vicinity within Area G then is determined from the best estimate of the effective diffusion coefficient, $D_{eff} \sim 15\ m^2/yr$, using Eqn.35, as

$$D_{ins}\ (Area\ G) \sim \frac{\theta\ D_{eff}}{H\ \varepsilon_a(\theta_a)} = \frac{0.01 \times 15}{1.56e\text{-}5 \times 0.36} \tag{37}$$

$$\sim 26700\ m^2/yr \sim 8.5 \times 10^{-4}\ m^2/s \sim 1 \times 10^{-3}\ m^2/s.$$

Implications

The binary diffusion coefficient for water vapor in air at this temperature is $2.5 \times 10^{-5}\ m^2/s$. The effective diffusion within the pore space observed at Area G is enhanced above the classical diffusion by a factor of $1 \times 10^{-3}/2.5 \times 10^{-5} = 40$ *times*. This is the value at Area G of the diffusion amplification factor, A_d, introduced in Eqn.21. This factor is expected to be closely related to the ratio of in-situ air permeability to the air permeability in unfractured core samples. As discussed previously, this ratio was found at Area G to vary from a factor of 4 in the lower units to a factor of 22 in Unit 2a and a factor of 16 in Unit 2b [9]. In the profiles at borehole G5 as shown in Fig.5, the ratio in the upper units (2b and 2a) is seen to be typically 10 or more and somewhat less, 3-4, below 60' depth. These observations are in agreement with the diffusion amplification found above and supports the notion that a fracture network at least throughout the upper layers enhances the in-situ diffusion and the air permeability.

Barometric or temperature fluctuations may also contribute towards the enhanced in-situ diffusion. They may contribute independently or synergistically towards enhancing the diffusion coefficient, depending upon the fluctuation mode numbers, periods, and effective transport distance over a single oscillation.

Barometric fluctuations with a diurnal or seasonal period penetrate deeply into the mesa (10s to 100s of meters). A simple model of diffusion resulting from barometric pumping at Area G was made previously [17], which led to the maximum (near surface) diffusion coefficient, D_{bp}, of

$$D_{bp} = \pi \frac{k_p}{\mu_a} \frac{\Delta p_s^2}{P_o} \tag{38}$$

where P_o is the ambient pressure, and Δp_s is the pressure mode amplitude at the ground surface. This maximum (near surface) diffusion coefficient was shown to be independent of mode number, and so the pressure mode

amplitude, Δp_s can be taken as a sum over individual modes. Using typical Area G parameter values, $k_p \sim 0.5x10^{-12} m^2$, $\Delta p_s \sim 10 mbar = 10^3 Pa$, $\mu_a \sim 2x10^{-5}$ $N{\cdot}s/m^2$, $P_o \sim 800 mbar = 0.8x10^5 Pa$ (Area G, Los Alamos is at 6500' elevation), this results in an estimate for the diffusion coefficient due to barometric pumping at Area G of

$$D_{bp} \sim 30\ m^2/yr\ . \tag{39}$$

This is the same magnitude as the best estimate derived from the field study, $15 m^2/yr$. It agrees within a factor of two, possibly related to an overestimate of the pressure fluctuation amplitude, Δp_s, but is in relatively good agreement considering the uncertainties as discussed below. Note that the mechanism implied in the derivation of this diffusion coefficient, D_{bp}, is barometric pumping through the pore matrix. Fractures are not included in obtaining the coefficient of this magnitude, although the permeability data suggests that the fracture network does play some contributing role to the in-situ diffusion. Therefore, it is likely that the barometric pumping in the pore space is actually smaller than the estimate in Eqn.39.

Temperature fluctuations are not expected to penetrate more than several meters into the mesa and should therefore have a minimal effect on the in-situ diffusion deep within the mesa. There might be a greater effect in the presence of a significant surface-connected fracture network, for which there is some evidence at Area G. The issues on both temperature and barometric pumping will be examined in greater detail in a subsequent followup study.

Analyses in the present study (e.g., as in Fig.13), found that the release time from the disposal shafts, τ, best fit the field data when the same value for τ was used at all the shafts. The newer shaft, #154 is lined with corregated steel, while the older shafts, #150 and 151, are unlined. In initial runs, the lined shaft was assigned a longer release time constant (slower release) and modest agreement with the field data was obtained. This is reflected in Fig. 11 showing the log results. In the comparisons of the data on linear scales, for example as depicted in Fig. 13, the characteristic tritium plume dimensions are easier to estimate. Here, the relative dimensions and magnitude of the tritium plumes around each shaft suggest that the better match to the field data (Fig.13) occurred for a shaft release value, τ, which was the same for each of the three shafts in the 3-D model. This suggests that the lined shafts and the unlined shafts have similar release rates, and the lined shafts do not provide additional barriers to the tritium diffusion into the surrounding tuff.

The absolute magnitude of the shaft release constant, τ, can be determined from field data such as the subsurface tritium moisture concentrations seen in Fig.4. The maximum value seen in the core sample moisture is about 10^7 pCi/m^3 or 10 Ci/m^3. This is a moisture concentration where the sample volume is that of the liquid phase, about 1% of the total

volume, and thus corresponds to about 0.1 Ci/m^3 tritium per total volume. The computational results from between the shafts 150 and 151 correspond to the location of the field profile in Fig.4 (top). The maximum computed tritium concentrations at this location were found to be 2 Ci/m^3 (calculated as a total volume concentration) when setting a value of $\tau = 50$ *years*. The solution is linear with $1/\tau$, so to correct the computation to the field result of 0.1 Ci/m^3, then value of τ required in the computation to match the field data is $\tau = 50yrs \times (2/0.1) \sim 1000$ *years*. This is the effective release time constant from the tritium waste packages.

The tritium moisture profiles in Fig.4 also provide a direct estimate of the attenuation length along a vertical axis due to the effective diffusion. The 'cleanest region' to determine an attenuation length in the profiles in Fig.4 is downward from the shaft bottom (at 60' ~ 20m). Over this region in both plots the e-folding length, L, is clearly in the range of $L \sim 8'$ *to* $10'$. This is coincidentally similar to the attenuation length used in Eqn.32 showing that for the 1-D spherical symmetry case, then the corresponding effective diffusion coefficient was 4 m^2/yr. Spherical geometry is probably a good approximation to the geometry when looking downward from the source at the disposal shaft bottom. Threfore, the effective diffusion coefficient in the region below the shaft bottom at ~ 60' is about 4 m^2/yr.

This is about 4 times smaller than the best estimate of the effective diffusion coefficient at Area G in Eqn.34, derived from diffusion in the upper most 60' of the tuff. The difference may be attributable to the large uncertainties (as in the following section), but suggests a real difference in the in-situ diffusion coefficient averaged over the depth from the surface to 60' compared to that for the depths below 60'. The observed decrease in fracture density at about 60' (at the unit 2b-2a interface) would support the finding that the diffusion coefficient is greater in the upper layers which are more fractured. The decrease in effective diffusion coefficient at depths > 60', is in line with the decrease in permeabilities from Units 2 to Units 1, and as seen in Fig.5.

The variation of tritium flux in time exhibits significant diurnal and annual variations as seen in the Field Data section. Good correlations with temperature were found. Tritium flux measurements used to characterize the tritium ground plume were made during the warmer part of the day and during the warmest season of the year, both tending to bias the sampled data above the annual mean values. When the quantitative magnitude of the flux data is important, as in estimating the actual emission releases of tritium from the disposal facilities, then the results should be corrected for these trends, for example by using the established temperature correlations. For the purposes of this study, the dimensions of the tritium plume will not vary greatly in time and so a time dependent correction is not needed in the present study.

The in-situ diffusion or dispersion coefficient is enhanced by about a factor of 40 over that expected by classical diffusion in a porous media with

the properties of the Bandelier Tuff. This enhanced transport is likely due to convective driven transport due to some combination of barometric and temperature fluctuations, along with possible coupling to transport in the fracture network in the upper layers of the mesa. It is assumed that the enhanced diffusion is due to oscillatory convective movements which act similarly on all gases and vapors. Refering back to Eqns.9-10, this may not be true for gases with different temperature dependences if temperature gradients are important. It is more likely that the barometric pumping of the total pore air volume is important at depth, which implies similar transport for any entrained species in the gas or vapor phase. The effective diffusion movement is then not dependent upon the molecular mass of the gaseous or vapor species. Therefore, the diffusion coefficient determined in this study is considered applicable to other gas or vapor species of interest at Area C.

Uncertainties

The net error in the in-situ diffusion coefficient in Eqn.35 can be evaluated rigorously from the propagation of errors [22]. The error in H is assumed small, error terms are assumed to be independent, and so the total error in D_{ins} is σ_{Dins}, approximately given as

$$\left(\frac{\sigma_{Dins}}{D_{ins}}\right)^2 = \left(\frac{\sigma_{ra}}{c_a}\right)^2 + \left(\frac{\sigma_\theta}{\theta}\right)^2 + \left(\frac{\sigma_{Deff}}{D_{eff}}\right)^2 . \qquad (40)$$

Unfortunately, the errors in each of the contributing factors are fairly large and difficult to quantify.

The two determination methods which assumed isotropic diffusion from point sources (spherical symmetry) located at the depths of the tritium waste packages produced two estimates of the effective diffusion coefficient, D_{eff}, with an arithmetic mean and deviation of $\sim 16m^2/yr \pm 9m^2/yr$ or geometric mean and deviations of $10m^2/yr \pm 4$, indicating a wide disparity in the estimates. The estimates from the two methods converge towards an intermediate value if the sources are assumed to be cylindrical. An exact assessment of the uncertainty would require a more complete analysis but is estimated here from a qualitative review of these analyses, and assuming that the effective geometry of the source is cylindrical. The expected value for the effective diffusion coefficient is $15m^2/yr$, and the actual value is most likely between $10m^2/yr$ and $20m^2/yr$. Qualitatively then, the effective diffusion coefficient is $D_{eff} = 15 \pm 5\ m^2/yr$, or with an error estimate of about 30%.

The moisture content varies considerably throughout the vertical profile as seen in Fig.3. In a detailed modeling effort, the actual moisture profile could be input to the model, however, in the present analysis, we are interested in an average value which is weighted in some manner for the

depths nearest the tritium source. To the extent the source is actually cylindrical, then weighting the vertical profile may in fact not be necessary. The estimate for the average moisture has been taken as $\theta \sim 0.01$. A detailed error estimate could be made from the data in Fig.3 or from Fig.4 (showing tritium, H3, concentrations and *H3/(vol% water)*). Again, for the present analysis, a qualitative judgement is made that the error in the mean moisture content is about 50%.

The error in the porosity correction, $\varepsilon_a[\theta_a]$ is also not known and estimated here to be about 30%. Refering back to Eqn.40, the total error for the in-situ diffusion coefficient is evaluated approximately as

$$\left(\frac{\sigma_{Dins}}{D_{ins}}\right)^2 = (0.3)^2 + (0.5)^2 + (0.3)^2 \sim 0.43 . \qquad (40)$$

This is an estimate of the uncertainty of the in-situ diffusion coefficient derived from this particular study at this particular location, and corresponds to a relative error, (σ_{Dins}/D_{ins}), of about 66%.

Added to this, there is additional uncertainty introduced if one applies this number to the diffusion of other gas or vapor species at other locations at Area G. An implication of the large diffusion amplification factor, $A_D \sim 40$, is that the diffusion coefficient does apply equally well to other species, so this extrapolation should introduce small errors. An implication of the moisture content near the tritium shafts being among the lowest values observed at Area G is that vapor flux is greatest at this location and therefore the in-situ diffusion here is likely to be a maximum compared to other locations throughout Area G. On the other hand, all locations at Area G are similarly dominated by vapor flux throughout an intermediate range in depth within the mesa [2] and should not exhibit widely disparate values of the in-situ diffusion coefficient. This variation is not quantifiable, but the in-situ diffusion estimate is likely to be within a factor of two of the correct value at other Area G locations, and as indicated, this estimate is probably on the high side of the actual value at other locations.

Additional factors contribute to the uncertainty in ways which are more difficult to quantify. Computational concentrations are only comparable to the field surface flux measurements if the evaporation rate is constant on the average throughout the region. This is a reasonable assumption in the sparsely vegetated area of this study, but remains to be demonstrated. This could be demonstrated with the available data from the tritium flux study [3].

Characteristic attenuation lengths are evaluated from the field results and from the numerical solutions assuming e-folding lengths, which is rigorously true only for the exponential solution valid for the instantaneous point source. The characteristic lengths may vary slightly in the actual

geometries with the integral functions which characterize the exact analytic solutions for the continuous source and in the different geometries.

Conclusions

Field measurements of tritium surface flux indicate the spatial extent of a tritium plume near the disposal shafts at Area G. The observed characteristic scale lengths are compared to model predictions in different geometries to determine a value for the effective tritium diffusion coefficient, D_{eff}, for the combined transport paths of tritiated water, $D_{eff} = 15 \pm 5\ m^2/yr$. Initally assuming spherical geometries, the diffusion estimates were disparate but in assuming cylindrical geometry the estimates from different comparisons converge and the final uncertainty in D_{eff} is estimated to be about 30%.

Transport analysis is used to relate this effective diffusion coefficient to the in-situ vapor phase diffusion coefficient of $D_{ins} \sim 1x10^{-3}\ m^2/s$. This value is about 40 times greater than expected by simple theory for porous media diffusion. Barometric pumping and the increased permeability of the fracture network in the upper layers of the tuff material surrounding the disposal shafts both appear to be contributing to the enhanced in-situ diffusion. There are several uncertain factors in the derivation of the insitu diffusion coefficient, which leads to an estimated uncertainty of about 70% or more in this value.

In the final analyses, the time scale for release from the disposal shaft, τ, was seen to provide a good match to the field data when the same value was used for all the shafts, lined or unlined. This implies that the newer lined shafts do not contain tritum significantly better than the older unlined shafts. This point should be examined in greater detail if it becomes an important issue for disposal operations. Comparison of model results to measurements of borehole core sample tritium moisture content indicates the effective time scale for tritium release from the waste package is about 1000 years.

The comparisons of field data with analytic and numerical solutions indicate that the source term geometry is not determined by the localized point sources corresponding to the largest inventory disposal packages but rather corresponds to a cylindrical geometry source of the disposal shaft. This implies that after release from the waste package, the tritium vapor diffuses within the shaft relatively fast compared to its slower diffusion from the shaft and through the surrounding subsurface tuff. Data suggests that the vapor diffusion coefficient derived at this study location is likely to be a maximum value, but within a factor of two, of a mean value across Area G. Analyses also suggest that the diffusion coefficient below 60' is smaller by about a factor of 4, than the value from this study, $D_{eff} = 15 \pm 5\ m^2/yr$.

Because the in-situ diffusion is significantly enhanced above the classical vapor diffusion, the diffusion coefficient derived in this study is considered to be applicable to other gas or vapor species of interest in the assessment of the performance of the disposal units at Area G. The diffusion value derived at this particular location is likely to be conservative and over estimate the average at Area G, but is likely to be within a factor of two.

Nomenclature

D_{eff} - effective diffusion coefficient (via all diffusion mechanisms) in the transport equation for the liquid phase concentration of tritium, C_{H3}.

nomenclature table pending referee requirements

Acknowledgment

This work was supported in part by the U.S. Department of Energy, Waste Management Programs, under the Area G Performance Assessment. Many RADIAN staff were instrumental in the tritium flux field study. R. Gilkeson provided the field data on in-situ air permeability, obtained in field tests by R. Lowry and the staff of SEA, Inc. Danial B. Stephens & Associates provided the core sample air permeability data. B. Gallaher and staff in the Water Quality and Hydrology Group provided the tritium profile data for boreholes NPH-8 and NPH-9.

References

[1] - D. Hollis, E. Vold, K. Birdsell, J. Turin, P. Longmire, E. Springer, W. Hansen, D. Krier, R. Shuman, "Performance Assessment of LANL TA-54, Area G, LLRW Disposal Facility - Preliminary Draft", Los Alamos National Laboratory, Los Alamos, NM, August, 1995.

[2] - E. L. Vold, "An Analysis of Vapor Phase Transport in the Unsaturated Zone with Application to a Mesa Top Disposal Facility, Part I", Los Alamos National Laboratory Report LA-UR-96-973, Los Alamos, NM, 1996.

[3] - B. Eklund, and E. Vold, "Measurement of Emission Fluxes from Technical Area 54, Areas G and L", final report 1/4 from RADIAN to LANL-CST-14 under DOE subcontract 6345L0014-31, Los Alamos National Laboratory Report, LA-UR-95-3891, Los Alamos, NM, 1995.

[4] - E.L. Vold, "Analysis of Liquid Phase Transport in the Unsaturated Zone at a Mesa Top Disposal Facility", Los Alamos National Laboratory Report, LA-UR-96-370, Los Alamos, NM, January, 1996.

[5] - W.E. Lowry, et.al., "Open borehole anemometry and air permeability measurements, Area G, TA-54", Science & Engineering Assoc. report on in-situ measurements at G-5, Santa Fe, NM, Jan.18, 1996.

[6] - D. B. Stephens and Associates, "Laboratory analysis of soil hydraulic properties of G-5 soil samples, report no. DBSA/3854/195-1", prepared for Los Alamos National Laboratory, Los Alamos, New Mexico, January 1995.

[7] - Rogers, D. B., and B. M. Gallaher, "The Unsaturated Hydraulic Characteristics of the Bandelier Tuff", 132 pp., Los Alamos National Laboratory Draft Report LA-12968-MS, May 1995.

[8] - P. M. Kearl, J. J. Dexter, and M. Kautsky, "Vadose zone characterization of Technical Area 54, waste disposal areas G and L, Los Alamos National Laboratory, New Mexico, Report 3: Preliminary assessment of the hydrologic system, Report GJ-44", Bendix Field Engineering Corp., March 1986a.

[9] - International Technology Corporation, "Hydrologic Assessment of Technical Area 54, Areas G and L, Los Alamos National Laboratory", Final Report, Docket Number NMHWA 001007, Los Alamos National Laboratory, Los Alamos, NM, March, 1987.

[10] - D.E. Broxton, G.H. Heiken, S.J. Chipera, F.M. Byers, Jr., "Stratigraphy, petrography, and minerology of Bandelier Tuff and Cerro Toledo deposits",

p.33 in Los Alamos National Laboratory report, LA-12934-MS, Los Alamos, NM, June, 1995.

[11] - D. Neeper, ?? revise to abstract/laur/conf95??, personal communication, ERM Golder Corp., Los Alamos, NM, January, 1996.

[12] - Abeele, W.V., Nyhan, J.W., "Emanation and dispersal of tritiated water from disposal shafts", *Nucl. and Chem. Waste Mngmt.*, 7, 217, 1987.

[13] - Environmental Protection Group, "Environmental Surveillance at Los Alamos during 1993" , Report LA-12973-ENV, Los Alamos National Laboratory, Los Alamos, NM, 1995.

[14] - D.E. Smiles, W.R.Gardner, R.K. Schulz, "Diffusion of tritium in arid disposal sites", Water Resources Research, v.31,n.6, p.1483, 1995.

[15] - J.R.Philip and D.A. de Vries, "Moisture movement in porous materials under temperature gradients", Trans., Amer. Geophysical Union, v38,n2, p222, 1957.

[16] - J. Bear, Dynamics of Fluids in Porous Media, American Elsevier, New York, 1972.

[17] - E.L. Vold, "A Brief Review of Environmental Transport of Tritium at the Los Alamos LLRW Disposal Facility", proceedings of the 16th Annual USDOE LLRW Management Conference, Phoenix, AZ, Dec. 1994, ed. Sandra Birk, Idaho National Engineering Laboratory, Idaho Falls, ID, 1995.

[18] - R.J. Millington, "Gas diffusion in porous media", Science, 130,p.100, 1959.

[19] - H.S.Carslaw and J.C.Jaeger, "Conduction of Heat in Solids", Oxford University Press, New York, 1959.

[20] - D.A. Anderson, J.C. Tannehill, R.H.Pletcher, "Computational Fluid Mechanics and Heat Transfer", Hemisphere Pub. Corp., New York, 1984.

[21] - D. Krier, P. Longmire, R. Gilkeson, H.J.Turin, "Geologic, Geohydrologic, and Geochemical Data Summary of MDA G, TA-54, LANL", Los Alamos National Laboratory Report LA-UR-95-2696, (see also App.2A to Ref.1), Los Alamos, NM, 1995.

[22] - Bevington, P.R., Data Reduction and Error Analysis for the Physical Sciences, McGraw Hill Book Co., New York, 1969.

Table I. Tritium inventory and disposal data - input for 3-D numerical model

shaft ID	H3 source (10^5 Ci)	year disposed	depth (est.ft)	Δt (yrs)[1]
shaft 154	1.2	'85	60	9
	0.7	'86	38	8
	1.3	'87	23	7
shaft 150	0.3	'77	60	17
	0.4	'78	45	16
	0.6	'79	38	15
	0.3	'80	23	14
shaft 151	0.3	'82	60	12
	0.6	'85	38	9
	0.66	'87	23	7

1. Δt is years from disposal to 1994 (the year of the field flux measurements)

Table II. Point source approximations for spherical geometry.

parameter	shaft 154	shaft 151	shaft 150	averages
L_g -ft- [1]	32 (± 33%) [3]	29 (± 57%) [3]	22 (± 11%) [3]	27.7 (± 18%) [3]
d_{eff} -ft-	35	25	35	
Δt_{av} -yr-	8	8	15	
L_s -ft- [2]	12.4	13.2	6.3	10.6 (± 36%) [3]

1. L_g -ft- average of field observations as discussed in text.
2. L_s-ft- computed from L_g and d_{eff} as discussed in text.
3. All errors are expressed as ± (the sample standard deviation divided by the sample mean)

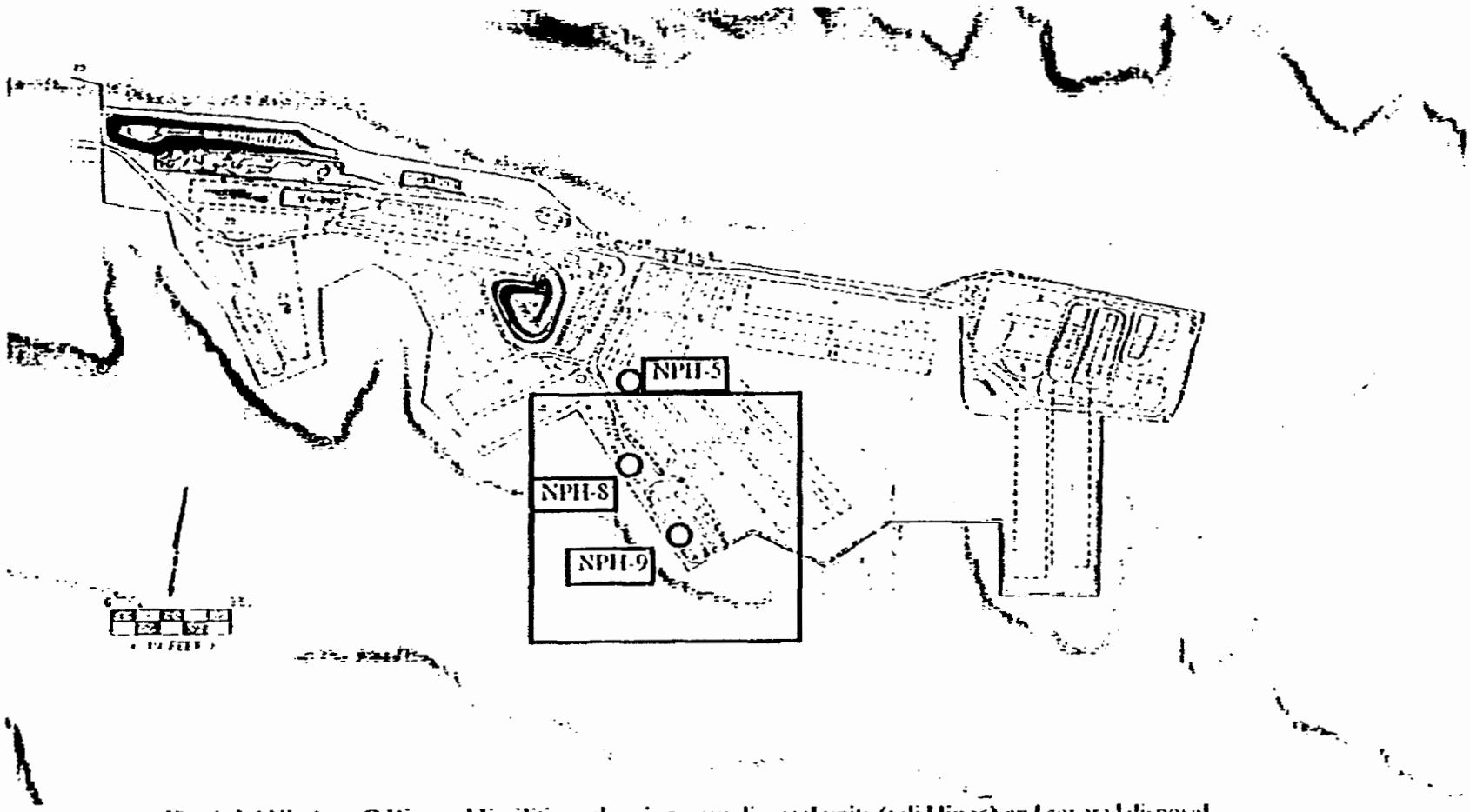

Fig. 1 LANL Area G Disposal Facilities - showing open disposal units (solid lines) and covered disposal units (dashed lines) and shafts (small cirles and boxes) imposed on terrain contours of the mesa top. The large box highlights the area around the tritium disposal shafts detailed in Figure 2 and in the surface flux result figures. Three monitor holes discussed in the text, NPH-5, NPH-8, and NPH-9 are shown.

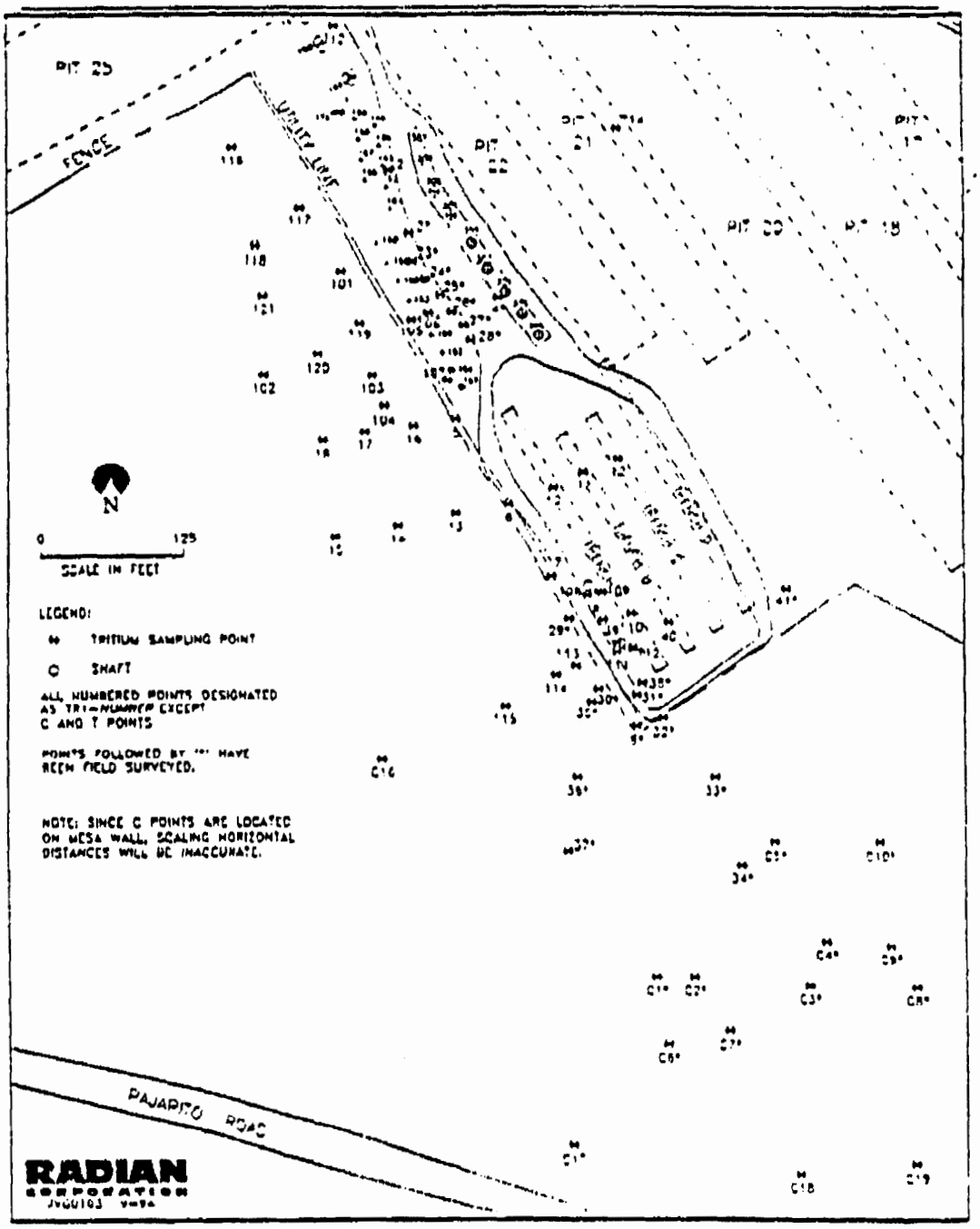

Fig. 2 Locations of tritium flux samplers in the vicinity of the high level tritium disposal shafts (area shown as box in Fig.1), including samples collected during 1993 and during 1994.

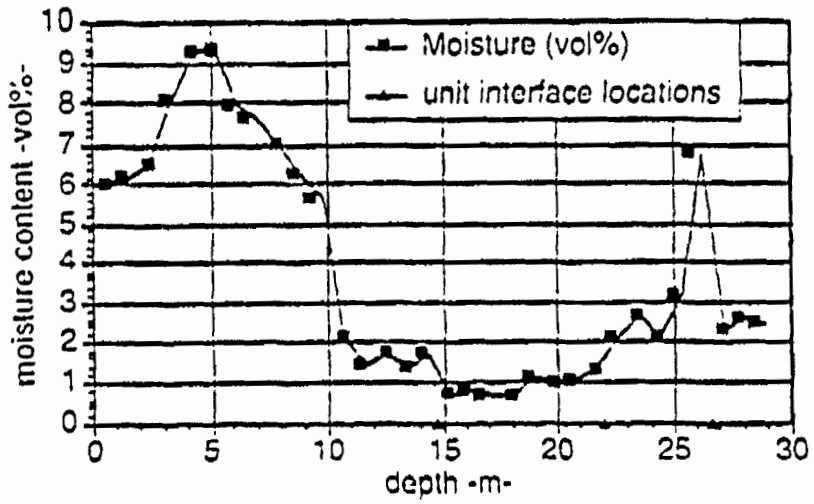

Borehole NPH-8 or ER-1110 (~ 50' E of tritium shaft 154)

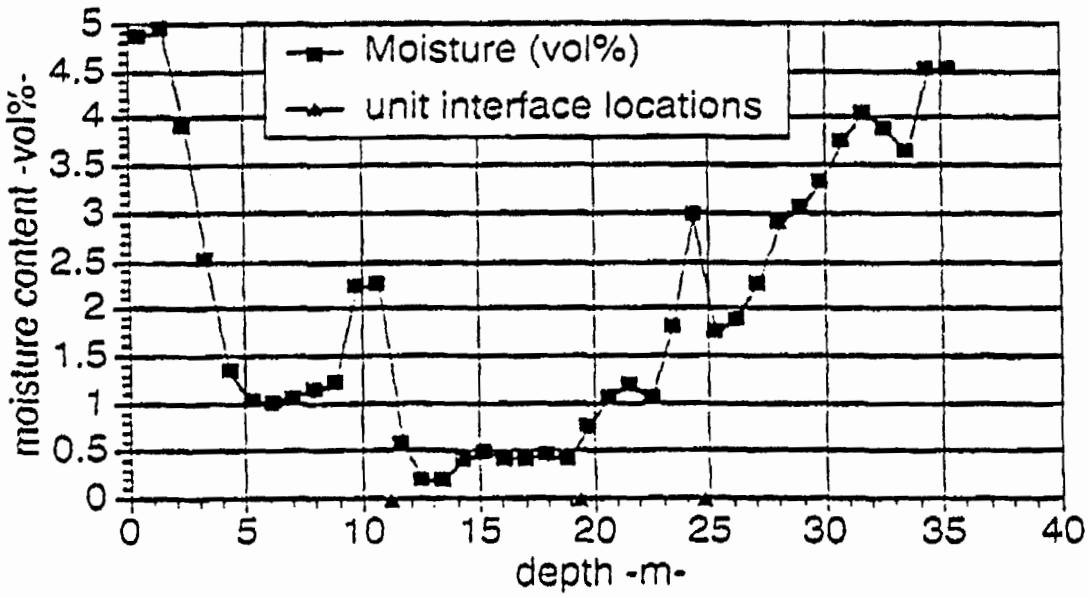

Borehole NPH-9 or ER- 1111 (between tritium shafts 150 and 151)

Fig. 3 Moisture profiles in the two boreholes in the immediate vicinity of the tritium shaft field.

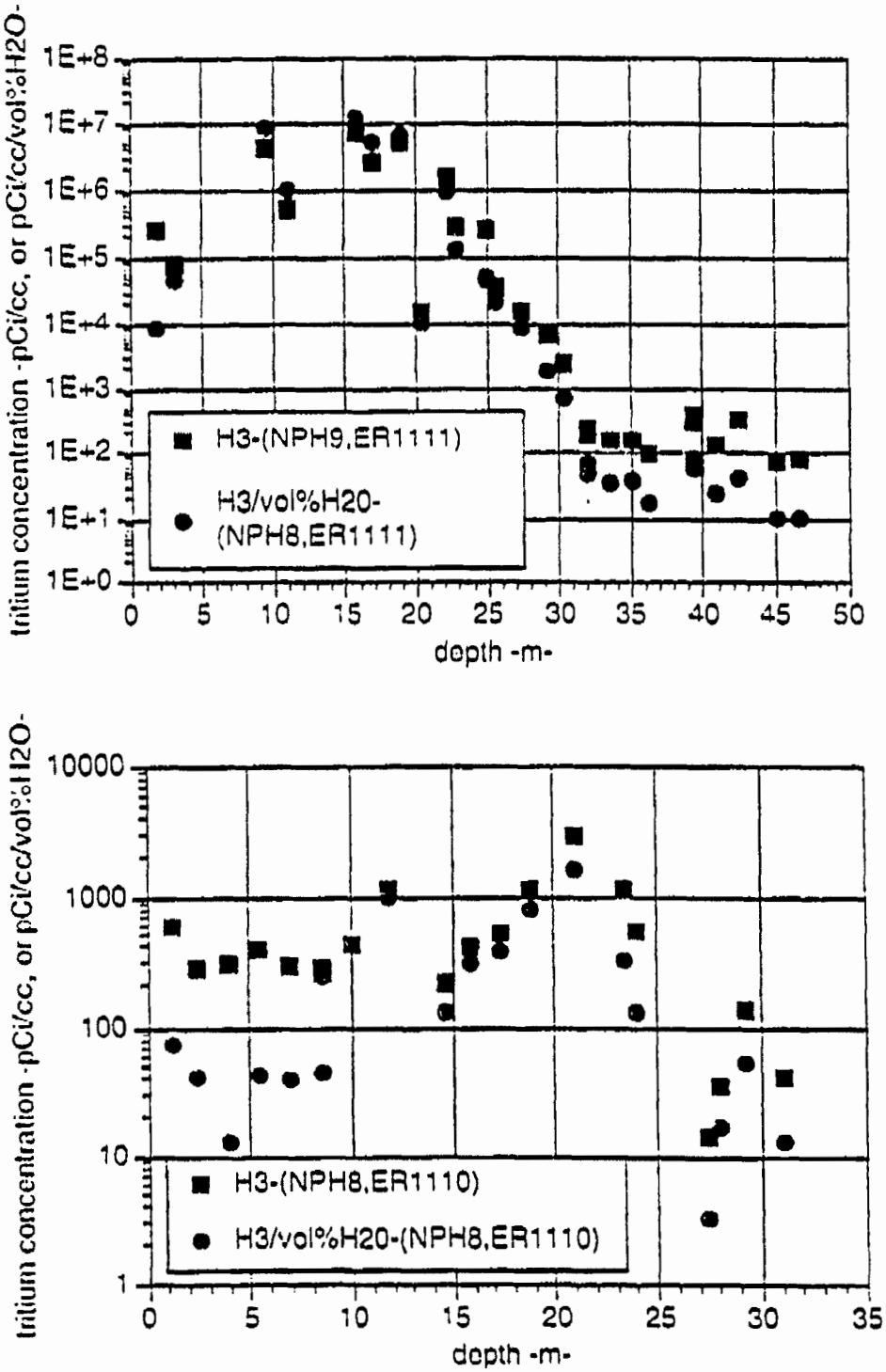

Fig. 4 Profiles of tritium concentration in borehole core moisture (labeled *H3*, in units of pCi/cc), and tritum concentration per volumetric moisture content (labeled *H3/vol%H2O*, in units of pCi/cc/vol%) in the two boreholes in the immediate vicinity of the tritium shaft field.

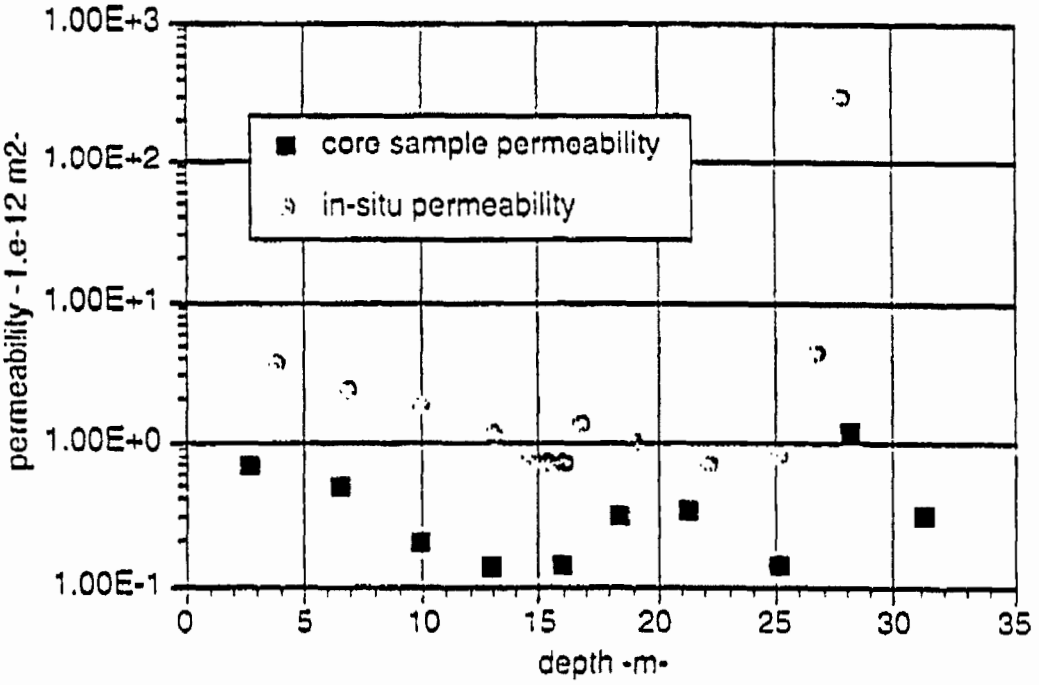

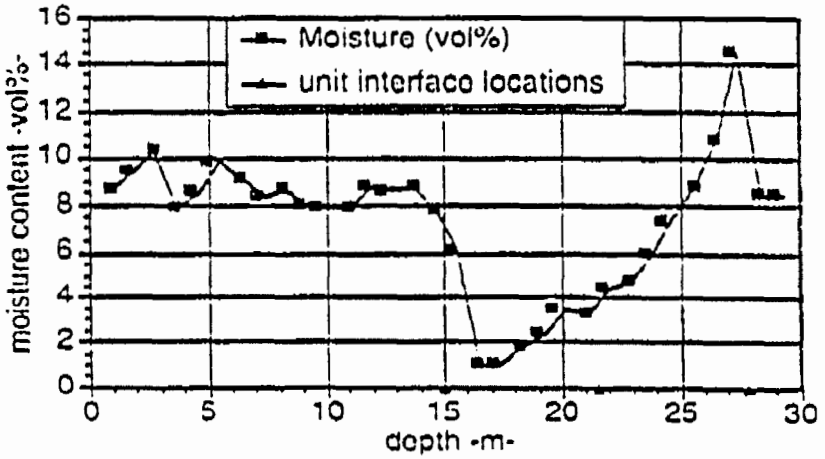

Fig. 5A (Top) Profiles of in-situ air permeability (data from Ref. 5) compared to core sample air permeability (data from Ref. 6).

Fig. 5B (Bottom) Moisture content profiles are shown for reference with the unit interface depths.

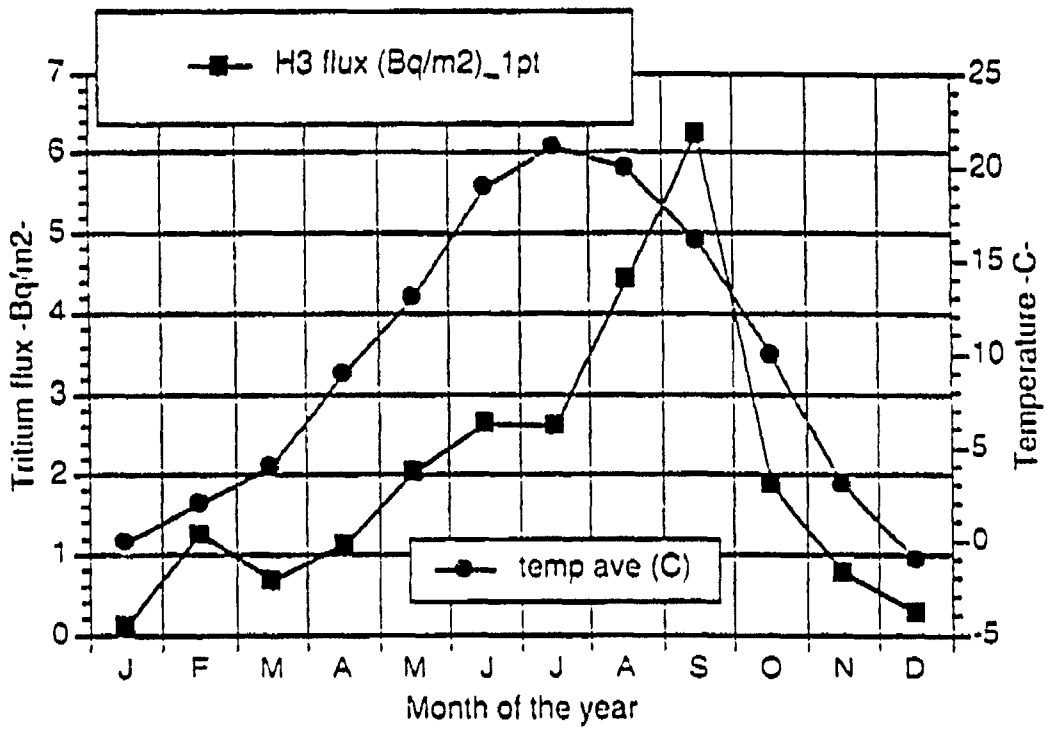

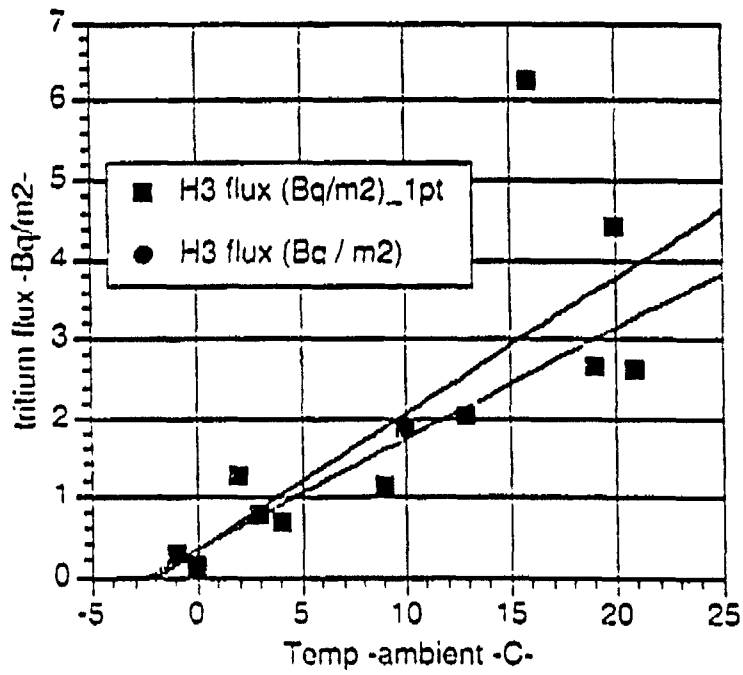

Fig. 6A (Top) Tritium surface efflux (data from Ref. 7) and monthly mean temperature shown verses month of the year.

Fig. 6B (Bottom) Linear correlation of monthly tritum flux with temperature for all points and for points with one 'out-lier' omitted.

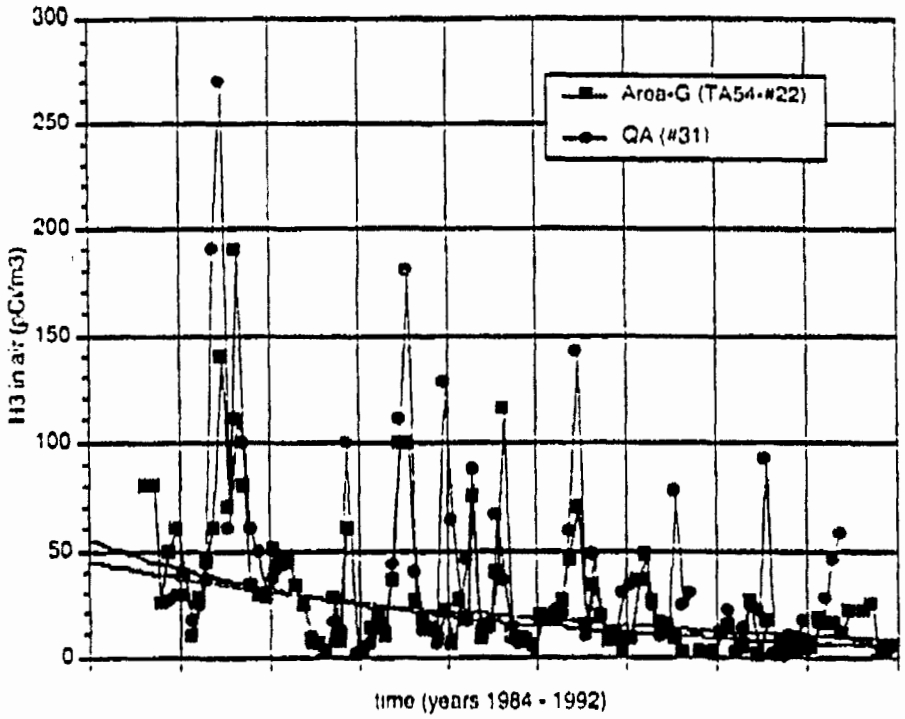

Fig. 7 Tritium in monthly integral air samples collected at two adjacent locations within Area G from late 1984 to 1992.

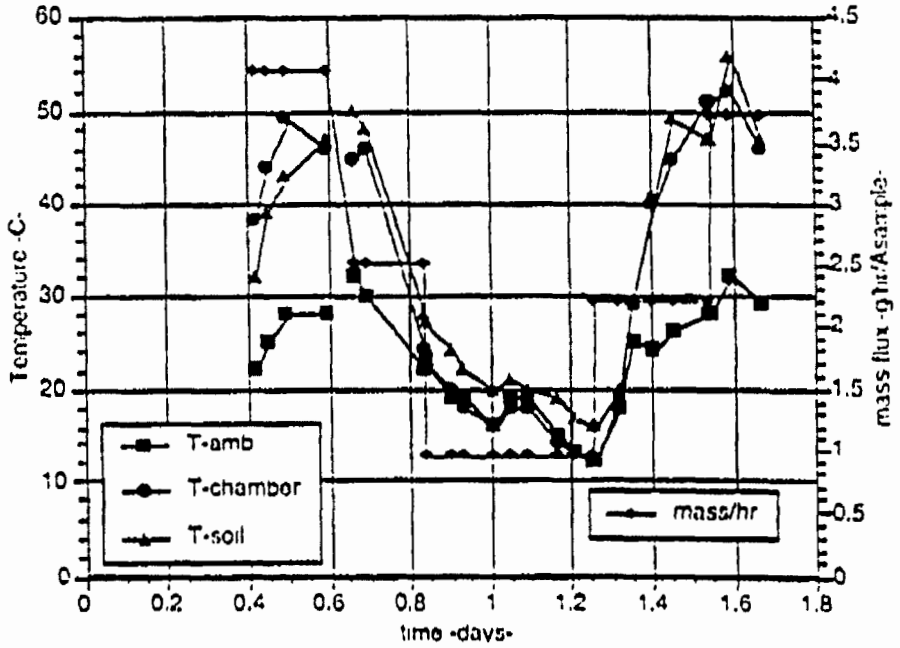

Fig. 8 Variation of temperatures and a relative measure of the water mass flux rate (evaporation rate) determined over a period of about 30 hrs, from late morning to the afternoon of the next day.

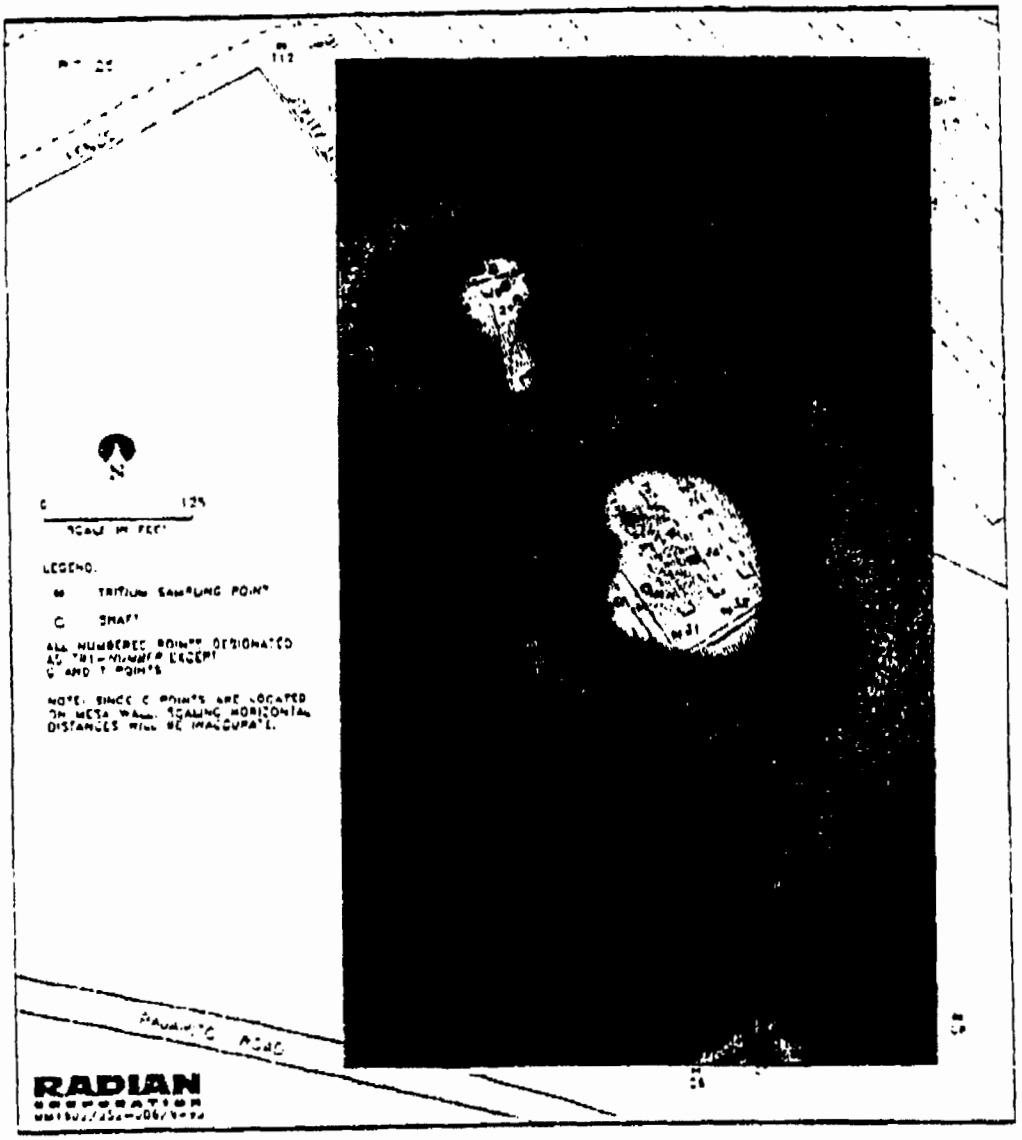

Fig. 9 Contour results of tritium flux in the vicinity of the high level tritium disposal shafts. Field results are scaled as log10(Flux) on the site map. This plot is interpolated from sample data taken at locations shown in the figure and includes only the samples collected from the first of the two years of sampling.

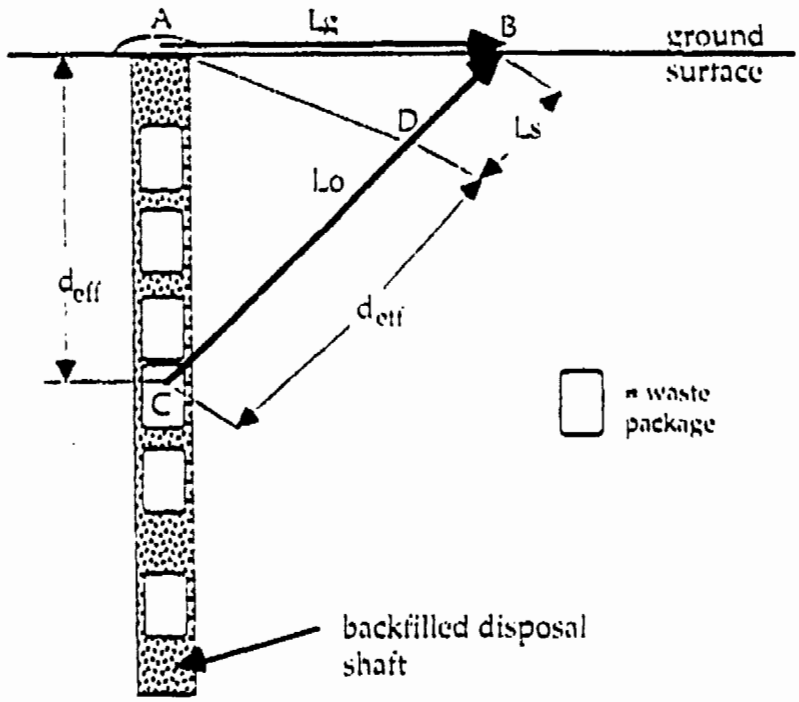

Fig. 10 Diagram of the disposal shaft and tritium waste package geometry used for the point source approximation in the 1-D spherical modeling.

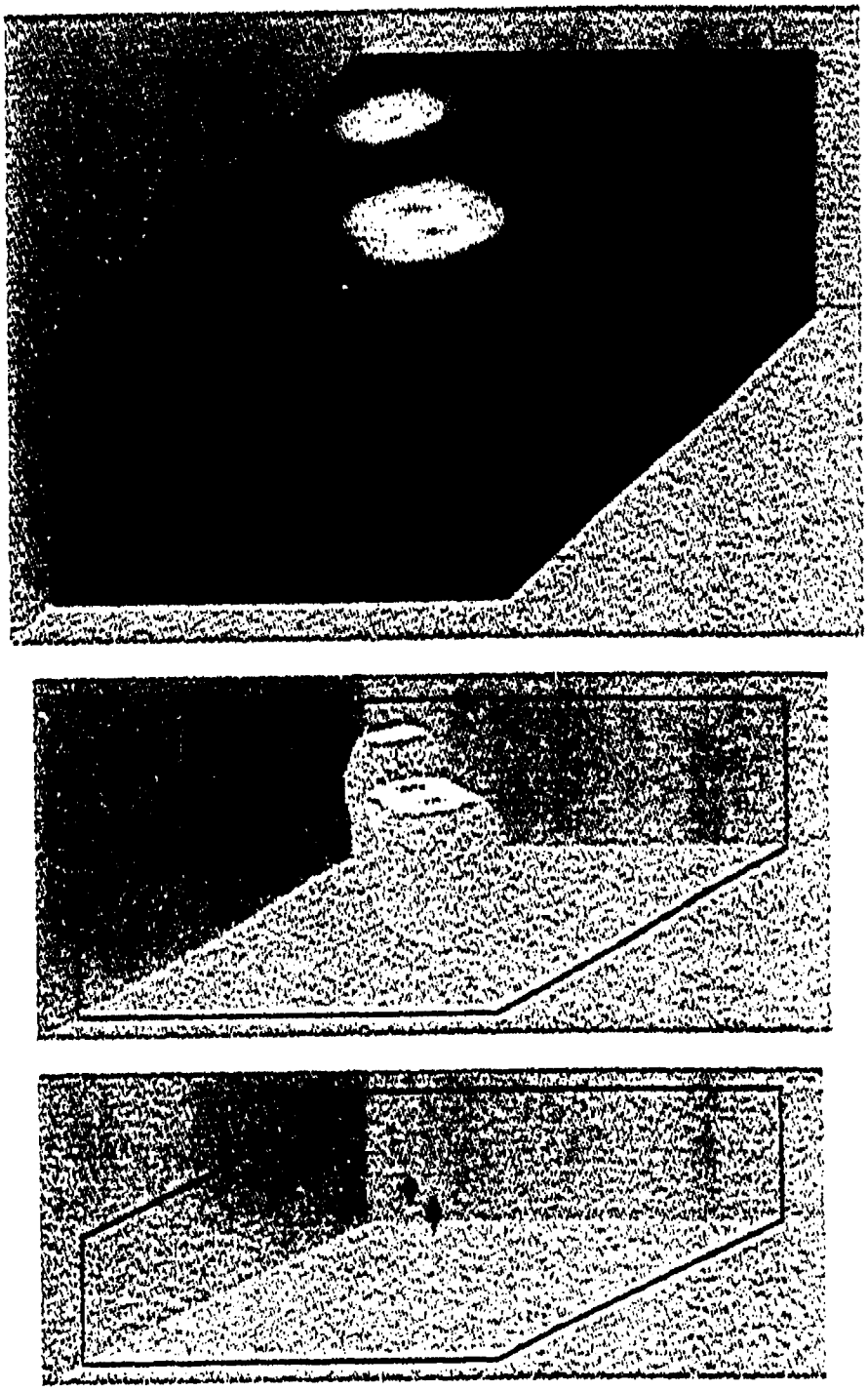

Fig. 11 Volume rendering of the computational results for tritium concentration. The top figure shows results on the surface of the entire computational volume while the lower figures show only contours of progressively greater concentrations, indicating the geometry of the disposal shaft and waste package sources.

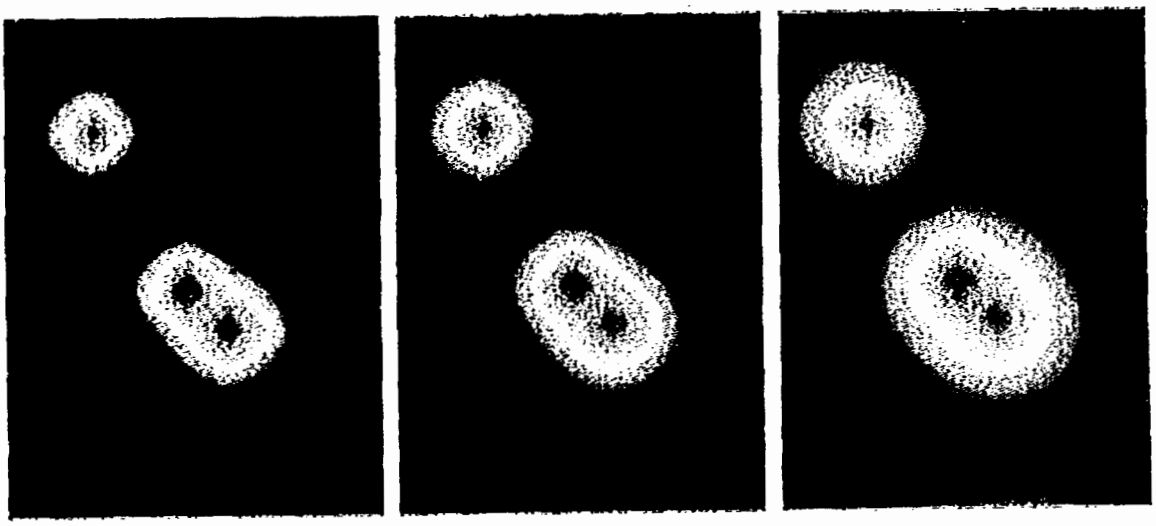

Fig. 12 Comparison of tritium contours computed at the ground surface for three values of the diffusion coefficient, D_{eff} = 50 ft^2/yr, 100 ft^2/yr and 250 ft^2/yr. The contours show *log10 of the tritium concentration* and indicate the area where the plume falls to background levels. The solution area shown is 600' (x) by 800' (y).

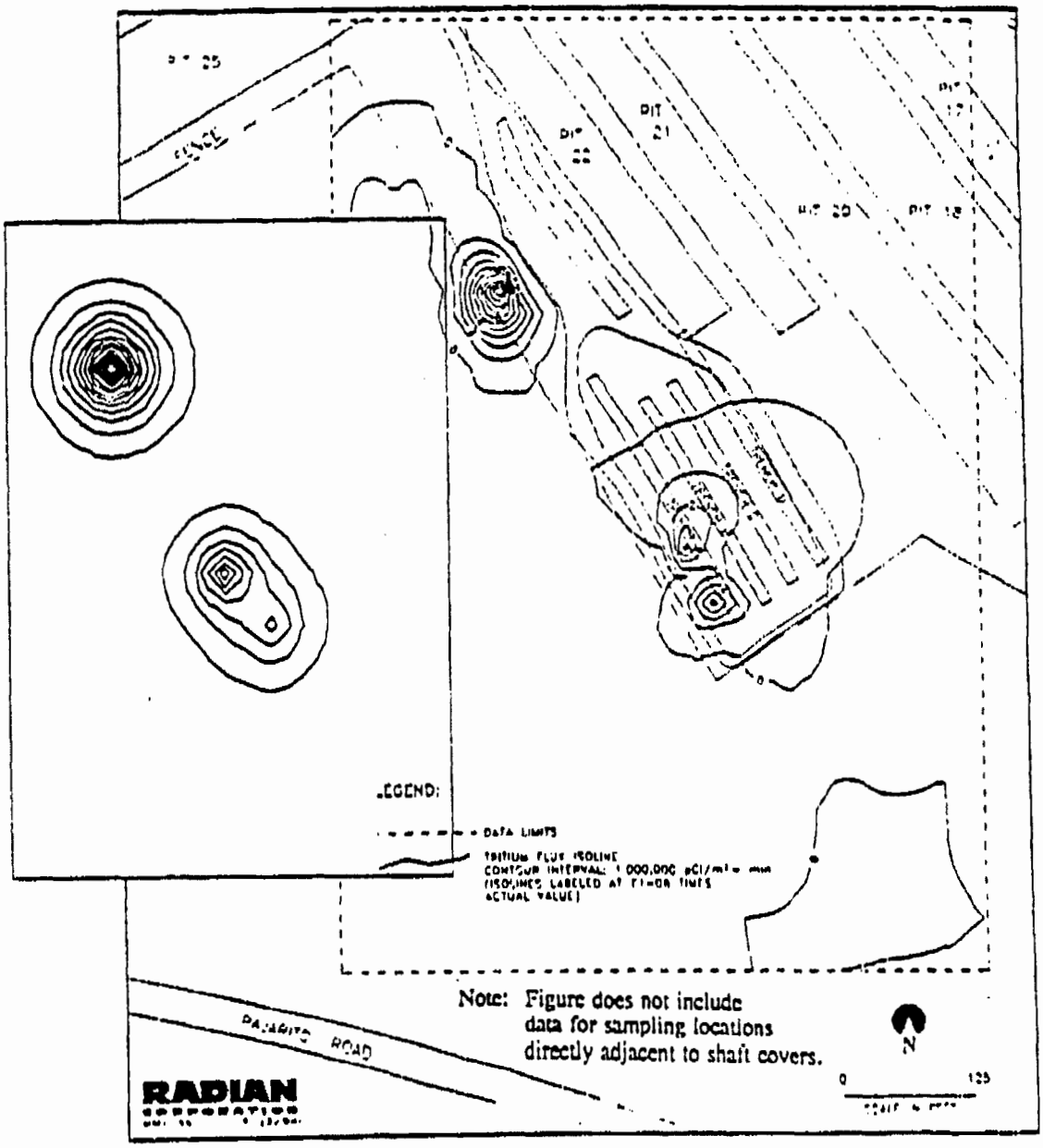

Fig. 13 Contour results of tritium flux in the vicinity of the high level tritium disposal shafts. Field results are shown on the site map, interpolated from sample data at the locations shown in Fig.2. The inset (left center) shows the computational results for the same area from the 3-D model. The inset window area is $(x,y) = 600' \times 800'$, approximately the same area as the dashed region on the map. The contour levels in each plot are relative and not quantitatively comparable between the field and the computational plots.

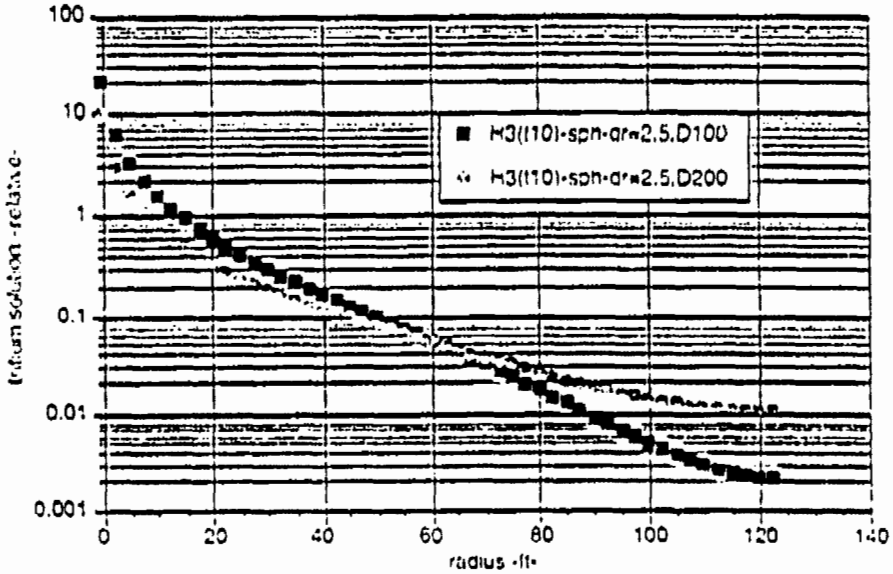

Fig. 14 Numerical solutions to the 1-D diffusion problem in spherical geometry compares spherical solutions for two values of the diffusion coefficient, $D = 100\ ft^2/yr$, and $D = 200\ ft^2/yr$, expected to bound the field results.

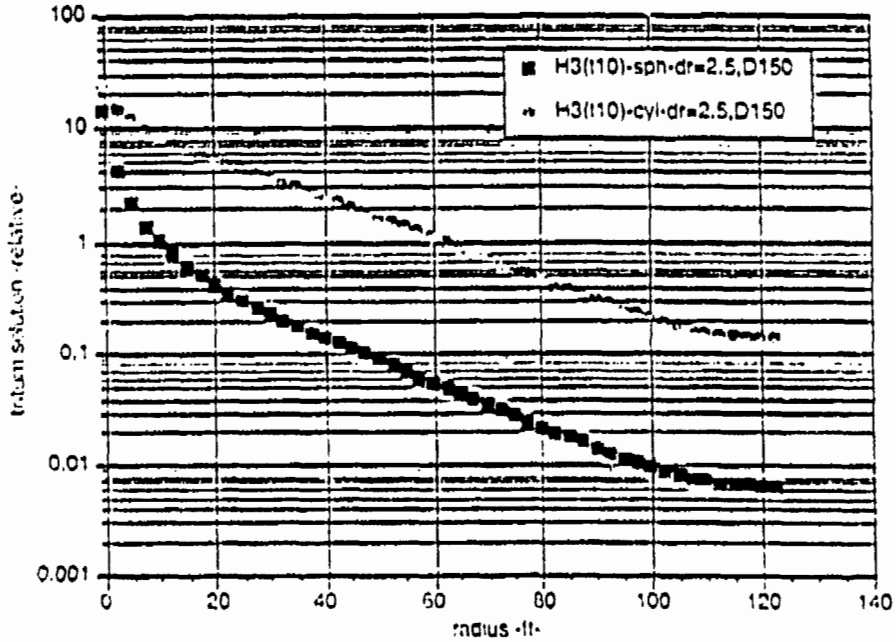

Fig. 15 Numerical solutions to the 1-D diffusion problem in spherical and in cylindrical geometry compares the spherical and the cylindrical geometry cases for the diffusion coefficient, $D = 150\ ft^2/yr$, expected to closely match the field results.